

# Monocrotophos Induces the Expression of Xenobiotic Metabolizing Cytochrome P450s (CYP2C8 and CYP3A4) and Neurotoxicity in Human Brain Cells

Vinay Kumar Tripathi<sup>1</sup> · Vivek Kumar<sup>2</sup> · Ankita Pandey<sup>3</sup> · Pankhi Vatsa<sup>3</sup> · Anupam Dhasmana<sup>4</sup> · Rajat Pratap Singh<sup>5</sup> · Sri Hari Chandan Appikonda<sup>6</sup> · Inho Hwang<sup>1</sup> · Mohtashim Lohani<sup>7</sup>

Received: 17 February 2016 / Accepted: 10 May 2016 / Published online: 20 May 2016  
© Springer Science+Business Media New York 2016

**Abstract** Expression of various cytochrome P450s (CYPs) in mammalian brain cells is well documented. However, such studies are hampered in neural/glial cells of human origin due to nonavailability of human brain cells. To address this issue, we investigated the expression and inducibility of CYP2C8 and CYP3A4 and their responsiveness against cyclophosphamide (CPA) and organophosphorus pesticide monocrotophos (MCP), a known developmental neurotoxicant in human neural (SH-SY5Y) and glial (U373-MG) cell lines. CPA induced significant expression of CYP2C8 and CYP3A4 in both types of cells in a time-dependent manner. Neural cell line exhibited relatively higher constitutive and inducible expression of CYPs than the glial cell line. MCP exposure alone could not induce the significant expression of CYPs, whereas the cells preexposed to CPA showed a significant response to MCP. Similar to the case of

CPA induced expressions, neural cells were found to be more vulnerable than glial cells. Our data indicate differential expressions of CYPs in cultured human neural and glial cell lines. The findings were synchronized with protein ligand docking studies, which showed a significant modulatory capacity of MCP by strong interaction with CYP regulators-CAR and PXR. Similarly, the known CYP inducer CPA has also shown significant high docking scores with the two studied CYP regulators. We also observed a significant induction in reactive oxygen species (ROS), lipid peroxides (LPO), micronucleus (MN), chromosomal aberration (CA), and reduction in reduced glutathione (GSH) and catalase following the exposure of MCP. Moreover, the expressions of apoptotic markers such as caspase-3, caspase-9, Bax, and p53 were significantly upregulated, whereas the levels of antiapoptotic marker, Bcl2, was downregulated after the exposure of MCP in both cell lines. These findings confirm the involvement of ROS-mediated oxidative stress, which subsequently triggers apoptosis pathways in both human neural (SH-SY5Y) and glial (U373-MG) cell lines following the exposure of MCP.

✉ Vinay Kumar Tripathi  
vinaytripathi2007@gmail.com

- <sup>1</sup> Department of Animal Science and Biotechnology, Chonbuk National University, Jeonju 561-756, Republic of Korea
- <sup>2</sup> Human Genome and Stem Cell Research Center, Department of Genetics and Evolutionary Biology, Biosciences Institute, University of Sao Paulo, Sao Paulo, SP, Brazil
- <sup>3</sup> In Vitro Toxicology Laboratory, CSIR-Indian Institute of Toxicology Research, Lucknow, India
- <sup>4</sup> Research Cell, Amity University, Lucknow, India
- <sup>5</sup> Department of Biochemistry, Dr. Ram Manohar Lohia Avadh University, Faizabad, India
- <sup>6</sup> Department of Molecular Genetics, L. V. Prasad Eye Institute, Hyderabad, India
- <sup>7</sup> Research and Scientific Studies Unit, Collage of Nursing and Allied Health Science, Jazan University, Jazan, Saudi Arabia

**Keywords** Xenobiotic metabolism · Cytochrome P450s · Human neural cells · Human glial cells · Monocrotophos · Apoptosis · Genotoxicity

## Introduction

Xenobiotic metabolizing enzymes and transporters (XMETs) are involved in biotransformation and detoxification of carcinogens, environmental toxins, and therapeutic drugs [1]. XMETs are highly expressed in the digestive tract and especially in the liver, the most important organ for central

metabolism [2]. Extra hepatic expression of these CYPs has also been found in the brain, lung, bladder, and blood [3–5].

Besides the liver and other peripheral organs, P450 isoforms are expressed in neural and glial cells of the brain. Their function and significance is a topic of high interest because most of the neuroactive drugs used in therapy today are not only substrates but also inducers of brain P450s. Brain P450s is differentially regulated by those in the liver [6]. The prosthetic heme group appears to be essential for correct membrane insertion and enzymatic functionality of brain P450s. Although not contributing to body's overall drug metabolism, brain P450s fulfils certain functions within specific cell types of the brain. In astrocytes of brains' border lines, P450 isoforms are expressed in very high levels. They form a metabolic barrier regulating drug influx, modulation of blood-flow regulation and also act as signaling enzymes in inflammation. In neurons, however, P450s apparently have different functions. In regions of brain such as hypothalamus, hippocampus, and striatum, they provide signaling molecules like steroids and fatty acids necessary for neural outgrowth and maintenance [7]. Induction of these P450s by neuroactive drugs can alter steroid hormonal signaling directly in drug target cells, which may cause clinically relevant side effects like reproductive disorders and sexual or mental dysfunction. The understanding of brain P450 function appears to be of major interest in long-term drug-mediated therapy of neurological diseases.

The CYP2C enzymes are expressed to varying extents in a number of extra hepatic tissues such as the kidney, gut, brain, heart, aorta, and lung [3, 8]. The CYP2C enzymes are clinically important to metabolize more than 20 % of all pharmaceutical drugs like rosiglitazone and the anticancer drug paclitaxel [9, 10]. CYP2C8/9 enzymes are also responsible for the hydroxylation of retinoic acid [11] and the CYP2C enzymes are important in the generation of biologically active molecules such as epoxyeicosatrienoic acids (EETs) and hydroxyeicosatrienoic acids (HEETs) from arachidonic acid in both liver and extra hepatic tissues [12].

The CYP3A subfamily enzymes play a major role in the metabolism of ~30 % of clinically used drugs for almost all therapeutic classes [9, 13]. The expression of CYP3A4 has been detected in cultured brain tumor cells of astrocytic origin (e.g., glioblastoma or astrocytomas) [14]. The active site of CYP3A4, which is large and flexible, accommodates and metabolizes many preferentially lipophilic compounds with comparatively large structures [15]. CYP3A4 is also an efficient steroid hydroxylase with an important role in the catabolism of several endogenous steroids, including testosterone, progesterone, androstenedione, cortisol, and bile acids. CYP3A4 metabolizes testosterone and estradiol [16, 17], both are neuroactive steroids that can influence mood, behavior, sexuality, memory, and cognition [18].

The hippocampus is a predominant site for the synthesis and action of testosterone and estradiol [19]. Therefore, induction of CYP3A4-mediated metabolism in this brain structure may have important consequences.

Organophosphate pesticides (OPs) are commonly used in agriculture worldwide. The primary mode of OP neurotoxicity is due to acetylcholinesterase (AChE) inhibition that increases cholinergic neurotransmission in central and peripheral nervous systems [20]. A part from being neurotoxic, organophosphate insecticides (OPIs) can exert toxic effects on many other tissues and organs. Toxicity of OPIs results in negative effects on many organs and systems such as the liver, kidney, nervous system, immune system, and reproductive system [21–23]. Neurotoxicity is dependent on the AChE levels that differ between brain regions which are inhibited to different extents by individual Ops [24].

Cytochrome P450s metabolizes the OPs in the brain and their metabolites causes more neurotoxicity than the parent compounds. The long-term exposure of cypermethrin (class II pyrethroid pesticide) modulates the expression of VMAT 2, CYP2E1, GSTA4-4, and lipid peroxidation [25]. OP-induced neurotoxicity is also associated with oxidative stress [25–27]. Cholinergic hyperactivity results in increased production of reactive oxygen species (ROS) and the free radical-mediated oxidative damage in brain [28]. The correlation between AChE inhibition and oxidative damage is unclear in OP poisoning. In the brain, for example, this correlation may be influenced by the dose, route of poisoning, and regional levels of AChE that are differentially inhibited by different Ops, among other factors that contribute to neurotoxicity. A study of oxidative stress in different regions of the brain over the course of OP poisoning would clarify the contribution of AChE inhibition to oxidative damage-induced neurotoxicity of these pesticides.

Our previous study showed that the neural (SH-SY5Y) and glial (U373-MG) cells had the constitutive and inducible expression of CYP1A1, CYP2B6, and CYP2E1 after the exposure of known inducers and monocrotophos (MCP). The induction level of CYPs was comparatively lower in MCP-exposed cells than cells exposed to classical inducers. Preexposure (12 h) of cells to classical inducers significantly added the MCP-induced CYP expression and activity. To extend our previous study, the expression and inducibility of CYP2C8 and CYP3A4 were investigated in cultured human brain neural (SH-SY5Y) and glial (U373-MG) cell lines. Xenobiotic metabolizing capabilities of cells were studied using cyclophosphamide and MCP. These studies were further stretched to investigate the MCP-induced apoptotic cell death in cultured neural (SH-

SY5Y) and glial (U373-MG) cells. MCP was selected as a model pesticide since it has been extensively used worldwide and is known for its neurotoxicity [29].

## Materials and Methods

**Reagents and Consumables** All the specified chemicals and reagents viz., monocrotophos (MCP) and cyclophosphamide (CPA), were purchased from Sigma (Sigma St Louis, MO, USA) unless otherwise stated. Culture medium DMEM/F-12, antibiotics, fetal bovine serum, and Trypsin-EDTA were purchased from Gibco BRL, USA. All the antibodies used in this study were procured from Chemicon International, USA. Culture wares and other plastic wares were procured commercially from Nunc, Denmark. Milli Q water (double-distilled, deionized water) was used in all the experiments.

**Cell Culture** Human neuroblastoma cell line SH-SY5Y and glioblastoma U373-MG cell lines used in the study were procured from American Type Culture Collection (ATCC), Manassas, USA, and maintained at the Department of Animal Science and Biotechnology, Chonbuk National University, Jeonju, Republic of Korea, as per the standard protocols. In brief, the cells were cultured in DMEM/F-12, supplemented with 10 % fetal bovine serum (FBS), 0.2 % sodium bicarbonate, 100 units/ml penicillin G sodium, 100 µg/ml streptomycin sulfate, and 0.25 µg/ml amphotericin B. Cultures were maintained at 37 °C in 5 % CO<sub>2</sub>-95 % atmosphere under high humid conditions. Medium was changed twice weekly, and cultures were passaged at a ratio of 1:6 once in a week. Prior to use in the experiments, cell viability was ascertained by Trypan blue dye exclusion assay. The cultures showing viability more than 95 % were used in all the experiments. All the experiments were done on the cells with passage 18–25 only.

**Identification of Noncytotoxic Doses of MCP and CPA** In the present investigations, known inducer of CYP2C8, CYP3A4 (CPA) and known neurotoxin (MCP), an organophosphate pesticide were used. CPA and MCP were dissolved in a DMEM/F-12 medium. Prior to using in the expression studies, noncytotoxic doses of the CPA and MCP were identified in SH-SY5Y (human neural cell line) and U373-MG (human glial cell line). Cytotoxicity assessment was done using standard endpoint, i.e., tetrazolium bromide (3-(4, 5-dimethylthiazol-2-yl)-2, 5-diphenyl tetrazolium bromide (MTT) assay as described earlier by us [30]. In brief, neural (SHSY-5Y) and glial (U373-MG) cells ( $1 \times 10^4$  cells/well) were seeded in 96-well tissue culture plates and incubated in the CO<sub>2</sub> incubator for 24 h at 37 °C. The medium was aspirated, and cells were exposed to medium containing either of CPA (0.5–8 mM) and MCP ( $10^{-3}$ – $10^{-7}$  M) for 24–96 h at

37 °C in 5 % CO<sub>2</sub>-95 % atmosphere under high humid conditions. Tetrazolium salt (10 µl/well; 5 mg/ml of stock in PBS) was added 4 h prior to completion of respective incubation periods. On the completion of incubation period, the reaction mixture was carefully taken out and 200 µl of culture grade DMSO was added to each well. The content was mixed well by pipetting up and down several times to dissolve it completely. Plates were then incubated for 10 min at room temperature, and color was read at 550 nm using Multiwell Microplate Reader (Synergy H1 Hybrid Reader, Bio-Tek, Winooski, VT, USA). The unexposed sets, and sets exposed to MnCl<sub>2</sub> ( $10^{-4}$  M), were also run parallel under identical conditions that served as basal and positive control, respectively.

## Experimental Design (Fig. 1)

**Transcriptional Changes** Transcriptional changes in the selected CYPs (2C8 and 3A4), CAR, and PXR were studied in both neural and glial cell lines exposed to various concentrations of CPA and pesticide-monocrotophos as described in experimental design. Transcriptional changes in the apoptotic genes like bax, bcl2, p53, and caspase-9/3 have been also carried out after the exposure of MCP in both the cell lines. Xenobiotics induced alterations in CYPs, receptors and apoptotic changes in the mRNA expression were expressed in relative quantification by comparing the data obtained from unexposed cells. The quantitative real-time PCR analysis was done following the protocol described earlier by Kashyap et al. [31]. In brief, total RNA was isolated from both experimental and unexposed control sets using GeneElute mammalian total RNA Miniprep Kit (Catalog No. RTN-70, Sigma-Aldrich, St. Louis, MO, USA). Total RNA (1 µg) was reverse transcribed into cDNA by SuperScript III first strand cDNA synthesis kit (Catalog No. 18080-051, Invitrogen Life Science, USA). Quantitative real-time PCR (RT-PCRq) assay reactions were carried out with 2× SYBR Green PCR master mix (Applied Biosystems, USA) using ABI PRISM 7900HT Sequence Detection System having software version 2.2.1 (Applied Biosystems, USA). Results were in relative to the expression of housekeeping gene, i.e., β-actin. Real-time reactions were carried out in triplicate wells for each sample.

## Preparation of Ligand Structures

Ligand file of CPA and MCP were downloaded in .mol format (Table 1) from ChemSpider Chemical Database. These files could not directly be used by Autodock 4.0 tools [32]; thus, they were converted into .pdb files using Discovery Studio Visualizer version 2.5.5. Discovery Studio, a software package of biological molecular design solutions, makes it easier to examine the properties of large and small molecules by

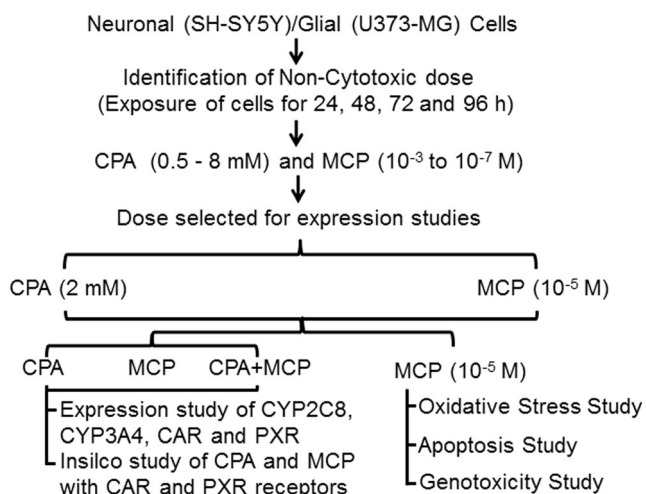


**Fig. 1** Experimental design of the study

computational chemists and computational biologists. Further, the ligands were submitted for minimization using Chimera version 1.5.3 using with Genetic Algorithm Steps 2000 and 0.5 grid units Optimized [33].

### Preparation of Protein Structures

The structure of proteins involved in this study human Constitutive Androstane Receptor (CAR), PDB ID-1XPV, and Human Pregnane X Receptor (PXR), PDB ID-2O9I, were obtained from RCSB Protein Data Bank. Published structures were edited to remove HETATM using Discovery Studio Visualizer (version 2.5.5). Chimera was used for energy minimization, removal of steric collision with the steepest descent steps 1000, steepest descent size 0.02 Å, conjugated gradient steps 1000, and the conjugate gradient step size 0.02 Å for the conjugate gradient minimization [34, 35].

### Docking Studies

Docking studies were performed by Autodock version 4.0 suits [36, 37]. Cygwin interface was used in the Microsoft Windows 7 professional Version 2002, Service pack 3, operating System on Intel (R) Core (TM) 2 Duo, CPU T6500 @ 2.10 GHz, 1.19 GHz, and 2.96 GB of RAM of Dell Machine. We implemented molecular docking methods followed by the searching of the best conformation of enzymes and complex compounds on the basis of binding energy. Water molecules were removed from the protein structures before docking and hydrogen atoms were added to all target proteins. Kollman united charges and salvation parameters were added to the proteins. Gasteiger charge was added to the ligands. Grid box was set to cover the maximum part of proteins and ligands. The values were set to  $60 \times 60 \times 60$  Å in X-, Y-, and Z-axes of grid point. The default grid points spacing was 0.375 Å. Lamarckian genetic algorithm (LGA) [38] was used

for proteins ligands flexible docking calculations. The LGA parameters like population size (ga\_pop\_size), energy evaluations (ga\_num\_generation), mutation rate, crossover rate, and step size were set to 150, 2,500,000, 27,000, 0.02, 0.8, and 0.2 Å, respectively. The LGA runs were set to 40 runs. All 40 conformations of proteins and complex ligands were obtained and analyzed for the interactions and binding energy of the docked structure using Discovery Studio Visualizer version 2.5.5.

**Western Blot Analysis** Translational changes in the apoptotic genes like bax, bcl2, p53, caspase-3, and caspase-9 have been carried out after the exposure of MCP in both neural and glial cell lines. The Western blot analysis was done following the protocol described earlier by us [31]. In brief, cells were pelleted and lysed using Cell Lytic™ M Cell Lysis Reagent (cat. no. C2978, Sigma-Aldrich, St. Louis, MO, USA) in the presence of protease inhibitor cocktail (cat. no. P8340, Sigma-Aldrich, USA). Protein estimation was done using BCA Protein Assay Kit (cat no. G1002, Lamda Biotech, Inc., St. Louis, MO, USA). Then, the denatured proteins (100 µg/well) were loaded and electrophoresed using 10 % Tricine-SDS gel [39]. Proteins were transferred on polyvinylidene fluoride (PVDF) membrane (cat. no. IPVH00010, Millipore, Billerica, MA, USA) by wet transfer method at 180-mA current for 3 h. Nonspecific binding was blocked with 5 % nonfat dry milk powder in TBST [20 mM Tris-HCl (pH 7.4), 137 mM NaCl, and 0.1 % Tween 20] for 2 h at 37 °C. After blocking, the membranes were incubated overnight at 4 °C with anti-protein primary antibodies specific for bax, bcl2, p53, caspase-3, and caspase-9 (1:1000, Chemicon International, Billerica, MA, USA), in blocking buffer (pH 7.5). The membranes were then incubated for 2 h at room temperature with secondary anti-primary antibody conjugated with horseradish peroxidase (Chemicon International, Billerica, MA, USA). Then, the blots were developed using Super Signal West Femto Chemiluminescent Substrate™ (Thermo Fisher Scientific, Waltham, MA, USA) and Bio-Rad Versa Doc™ Imaging System 4000 (Bio-Rad, Philadelphia, PA, USA). The densitometry for protein specific bands was done in Gel Documentation System (Alpha Innotech, San Leandro, CA, USA) with the help of AlphaEase™ FC Stand Alone V.4.0 software. β-Actin was used as internal control to normalize the data. MCP-induced alterations are expressed in relative term fold change in expression by comparing the data with respective unexposed controls.

### Oxidative Stress Analysis

**Estimation of ROS Levels** Estimation of MCP-induced ROS generation was carried out following the standard protocol of Kashyap et al. [31]. In brief, SH-SY5Y and U373-MG cells

**Table 1** Assessment of binding affinities and biomolecular interactions of CPA and MCP with CAR and PXR

S. no.	Protein's name	PDB	Name of ligand	Binding energy (kcal/mol)	Inhibition constant (Ki)	Residues making hydrophobic contacts	Residues involved in hydrogen bonding	Hydrogen bond distance (Å)
1	Constitutive androstane receptor (CAR)	1XVP	Cyclophosphamide (CPA)	-5.35	119.48 $\mu$ M	Phe132, Leu157, His160 Phe161, Ile164, Met168 His203, Leu206, Phe217 Cys219, Tyr224, Thr225 Asp228, Gly229, Val232 Leu242, Phe243	ND	ND
2	CAR	1XVP	Monocrotophos (MCP)	-4.39	602.37 $\mu$ M	Phe132, Phe161, Ile164 Leu206, Phe217, Cys219 Tyr224, Thr225, Asp228 Gly229, Val232, Phe234 Phe238, Leu239, Leu242 Phe243	ND	ND
3	Pregnane X receptor (PXR)	2O9I	CPA	-5.32	126.05 $\mu$ M	Leu209, Val211, Met243 Met246, Gln285, Phe288 Trp299, Tyr306, Met323 Leu324, His327	1)A:GLN285:HE22 - :UNK1:O5 2):UNK1:H19 - A:GLN285:OE1	1) 2.5 Å 2) 2.5 Å
4	PXR	2O9I	MCP	-4.69	363.71 $\mu$ M	Leu209, Val211, Met243 Met246, Gln285, Phe288 Trp299, Cys301, Tyr306 Met323, Leu324, His327	1) :UNK1:H19 - A:GLN285:OE1	1) 2.5 Å
5	CAR-CPA complex		MCP	-5.34	121.56 $\mu$ M	Phe132, Phe161, Ile164 Asn165, Met168, Val169 Val199, Cys202, His203 Leu206, Phe217, Cys219 Tyr224, Asp228, Gly229 Val232, Phe234, Phe238 Leu242, Phe243, Ile322 Tyr326, Leu343	ND	ND
6	PXR-CPA complex		MCP	-5.47	97.27 $\mu$ M			1)2.5 Å

**Table 1** (continued)

S. no.	Protein's name	PDB	Name of ligand	Binding energy (kcal/mol)	Inhibition constant (Ki)	Residues making hydrophobic contacts	Residues involved in hydrogen bonding	Hydrogen bond distance (Å)
						Leu209, Val211, Met243 Gln285, Phe288, Trp299 Tyr306, Met323, Leu324 His327	1)A:GLN285:HE22 - :UNK1:O5 2);UNK1:H19 - A:GLN285:OE1	

( $10^4$  cells/well) were seeded in 96-well black-bottomed culture plates and allowed to adhere for 24 h under a 5 % CO<sub>2</sub>, 95 % atmosphere at 37 °C. Both cell types were exposed with MCP ( $10^{-5}$  M) for 3, 6, 12, and 24 h. Following exposure, cells were reincubated with 2,7-dichloro-dihydrofluorescein diacetate [DCFH-DA (20 μM)] for 30 min at 37 °C. The reaction mixture was then replaced with 200 μl of PBS per well. The plates were kept on a rocker shaker platform for 10 min at room temperature in the dark, and fluorescence intensity was measured using a multiwell microplate reader (Synergy H1 Hybrid Reader, Bio-Tek, Winooski, VT, USA) at an excitation wavelength of 485 nm and emission wavelength of 528 nm. The data are expressed as percent of unexposed control.

**Estimation of GSH Levels** Glutathione (GSH) levels were assessed following the exposure of MCP ( $10^{-5}$  M) to SH-SY5Y and U373-MG cells for 3, 6, 12, and 24 h using commercially available kit (Glutathione Detection Kit, catalog no. APT 250, Chemicon, Billerica, MA, USA). In brief, following MCP exposures, cells were collected by centrifugation at 7000g for 2 min at 4 °C and lysed in lysis buffer. The samples were centrifuged again at 12,000×g for 10 min at 4 °C, and the supernatant was collected. To estimate the GSH levels, the lysed samples (90 ml/well) were transferred to 96-well black-bottomed plates and mixed with freshly prepared assay cocktail (10 ml) and read at excitation wavelength 380 nm and emission wavelength 460 nm using multiwell microplate reader (Synergy H1 Hybrid Reader, Bio-Tek, Winooski, VT, USA) after the incubation of 1–2 h.

**Estimation of LPO Levels** Lipid peroxidation (LPO) was performed using the thiobarbituric acid reactive substances (TBARS) protocol [40]. In brief, SH-SY5Y and U373-MG cells ( $10^5$  cells/well) were seeded in six-well culture plates and allowed to adhere for 24 h under a 5 % CO<sub>2</sub>, 95 % atmosphere at 37 °C. Both cells were exposed with MCP ( $10^{-5}$  M) for 3, 6, 12, and 24 h. After completion of the exposure time period, the cells were collected by centrifugation and sonicated in ice-cold potassium chloride (1.15 %) and centrifuged for

10 min at 3000×g. The resulting supernatant (1 ml) was added to 2 ml of thiobarbituric acid reagent (15 % TCA, 0.7 % TBA, and 0.25 N HCl) and heated at 100 °C for 15 min in a water bath. Samples were then placed in cold and centrifuged at 1000×g for 10 min. Absorbance of the supernatant was measured at 535 nm. The data are expressed as percent of unexposed control.

**Estimation of Catalase Levels** The experimental setup for catalase activity was quite similar to the LPO. The activity was measured using commercially available kit for catalase activity (catalog no. 707002; Cayman Chemicals, Ann Arbor, MI, USA) following the protocol provided by manufacturer. In brief, SH-SY5Y and U373-MG cells ( $10^5$  cells/well) were seeded in six culture plates and allowed to adhere for 24 h under a 5 % CO<sub>2</sub>, 95 % atmosphere at 37 °C. Both cells were exposed to MCP ( $10^{-5}$  M) for 3, 6, 12, and 24 h. Following the completion of exposure periods, the cells were collected by centrifugation at 1000×g for 10 min at 4 °C and sonicated in 1.0 ml cold buffer (50 mM potassium phosphate, pH 7.0, containing 1 mM EDTA). Then, centrifuged at 10,000×g for 15 min at 4 °C and collected the supernatant for assay. Then, 100 μl of assay buffer (supplied in the kit), 30 μl of methanol, and 20 μl of sample were mixed in the 96-well plate. Reaction was initiated by adding 20 μl of hydrogen peroxide (0.882 M) and incubated in shaker for 20 min at room temperature. Reaction was stopped by adding 30 μl of potassium hydroxide. Then, chromogen (30 μl) was added and incubated for 10 min followed by addition of potassium periodate (10 μl). The plates were kept at room temperature for 5 min and read at 540 nm using multiwell microplate reader (Synergy H1 Hybrid Reader, Bio-Tek, Winooski, VT, USA).

**Translocation Studies** Translocation of Bax protein from cytosol to mitochondria and cytochrome-c from mitochondria to cytosol due to MCP-induced mitochondrial membrane permeabilization was studied by Western blotting using specific anti-Bax (Santa Cruz, Dallas, TX, USA) and anti-cytochrome-c primary antibodies (Cell Signalling Technology Inc., Danvers, MA, USA). After the exposure of

cells to MCP ( $10^{-5}$  M) for 24 h, cells were harvested and processed for isolation of mitochondrial and cytosolic fraction using the protocols of Kashyap et al. [30]. The cross-contamination of cytosolic protein in the mitochondrial fraction and vice versa was also assessed by running separate blots using antibodies specific to mitochondria and cytosolic proteins.

**Activity of Caspase-9 and Caspase-3** MCP-induced alterations in the activity of caspase-9 and caspase-3 were monitored using kits (catalog no. K119 and K106, BioVision, Milpitas, CA, USA, respectively). Following MCP exposure, cells were pelleted, resuspended in prechilled extraction buffer (50  $\mu$ l), and incubated for 10 min on ice. Then, the samples were centrifuged at 500g for 5 min, and the clear supernatant (50  $\mu$ l per well) was transferred to black-bottomed 96-well culture plates for caspase-9, and clear plates for caspase-3. Assay buffer (50  $\mu$ l) and substrate conjugate (10  $\mu$ l) for caspase-9 and (5  $\mu$ l) and caspase-3 were added and mixed well. Immediately after the completion of 2 h of incubation at 37 °C in the dark, contents were thoroughly mixed and read for fluorescence at 400-nm excitation and 505-nm emission wavelengths for caspase-9, and for absorbance at 400 nm for caspase-3. The values of exposed groups were compared with unexposed control sets, and the data were expressed as a percent of control.

### Genotoxicity Analysis

**Micronucleus Assay** MN assay was carried out using standard protocol of Srivastava et al. [41]. Briefly, SH-SY5Y and U373-MG cells were grown on cover slips placed in eight-well plates in DMEM/F-12 medium. The cells were exposed to  $10^{-5}$  M concentration of MCP; cells were incubated up to 43–44 h in fresh medium and blocked for cytokinesis using cytochalasin-B (3  $\mu$ g/ml). Cells were then harvested by hypotonic buffer (0.075 M KCl) for 5–10 min at 37 °C and fixed in Carnoy's fixative (methanol/acetic acid, 3:1). Finally, cells were dropped onto slides and stained with 5 % Giemsa in phosphate buffer (pH 6.8) for 15–20 min and mounted with DPX for microscopic examination. A minimum of 1000 binucleated cells with well-defined cytoplasm in each slide was scored for the presence of MN using a Nikon Eclipse 80i upright microscope attached to a Nikon digital CCD cool camera (Model DS-Ri1 of 12.7 Megapixel). Data presented for MN are the mean of three slides.

**Chromosomal Aberration Assay** SH-SY5Y and U373-MG cells were cultured in DMEM/F-12 medium in 25-cm<sup>2</sup> flasks, and the cells were exposed to  $10^{-5}$  M concentration of MCP. Colcemid (0.15  $\mu$ g/ml final concentration) was added 4 h prior to harvest the cells. After the compilation of 4 h exposure of colcemid, the medium was aspirated and the cells were

washed with Hank's balanced salt solution. After that, the cells were given a hypotonic shock in potassium citrate (0.8 %) for 30 min. Finally, cells were fixed in cold fixative (methanol/acetic acid, 5:2 ratios). Cells were dropped on clean slides, dried, and stained in 5 % Gurr's Giemsa. The cells were scored for the presence of CA using a Nikon Eclipse 80i upright microscope attached to a Nikon digital CCD cool camera (Model DS-Ri1 of 12.7 Megapixel). Data presented for CA are the mean of three slides.

**Statistical Analysis** The results are expressed as mean and standard error of means (mean  $\pm$  SE) for at least three experiments. One-way ANOVA followed by post hoc Dunnett's test was employed to detect differences between the groups of treated and control.  $P < 0.05$  was taken to indicate significant differences.

## Results

**Cytotoxicity Assessment** Both neural and glial cells responded significantly to CPA and MCP in a dose-dependent manner. However, the variation in response between cell types was not statistically significant (Fig. 2 a–d). Cells exposed to CPA concentrations (0.5–2 mM) were found safe in all the exposure periods, i.e., 24–96 h. Whereas, higher concentrations of CPA, i.e., 4 and 8 mM, caused gradual reduction in percent cell viability, which reaches to significant levels at the exposure period of 48 and 96 h. Neural cells showed  $49.88 \pm 3.21$  to  $24.79 \pm 2.26$  %, and glial cells showed  $47.94 \pm 4.69$  to  $26.96 \pm 2.26$  % cell viability up to 96 h (Fig. 2a, b). There was a gradual decrease in the percent cell viability of those cells exposed to MCP ( $10^{-7}$ – $10^{-5}$  M) for the period 24–96 h. MCP exposure at  $10^{-4}$  and  $10^{-3}$  M was significantly cytotoxic even at 24 h, and the magnitude was increased with the extended exposure period, i.e., 48, 72, and 96 h (Fig. 2c, d).

**Transcriptional Changes in CYPs (CYP2C8 and CYP3A4) and Receptors (CAR and PXR)** Neural cells showed a significant gradual increase in the expression of CYP2C8 after the exposure to CPA (2 mM) for 1, 3, 6, and 12 h, i.e.,  $2.76 \pm 0.08$ -,  $4.92 \pm 0.44$ -,  $7.48 \pm 0.070$ -, and  $11.64 \pm 1.12$ -fold of control, respectively. Cells also showed significant induction in the expression of CYP2C8 when they were exposed to MCP for 6 and 12 h; however, the magnitude of induction was comparatively lower to that of CPA exposed cells. A preexposure of CPA for 12 h showed significant additive effect in the expression of mRNA of CYP2C8 in the cells exposed to MCP for 1, 3, 6, and 12 h, i.e.,  $13.62 \pm 1.25$ -,  $16.84 \pm 1.55$ -,  $21.77 \pm 1.84$ -, and  $26.56 \pm 1.58$ -fold of control, respectively. The trend of upregulation in the expression of mRNA of CYP2C8 in glial cells was similar to that of

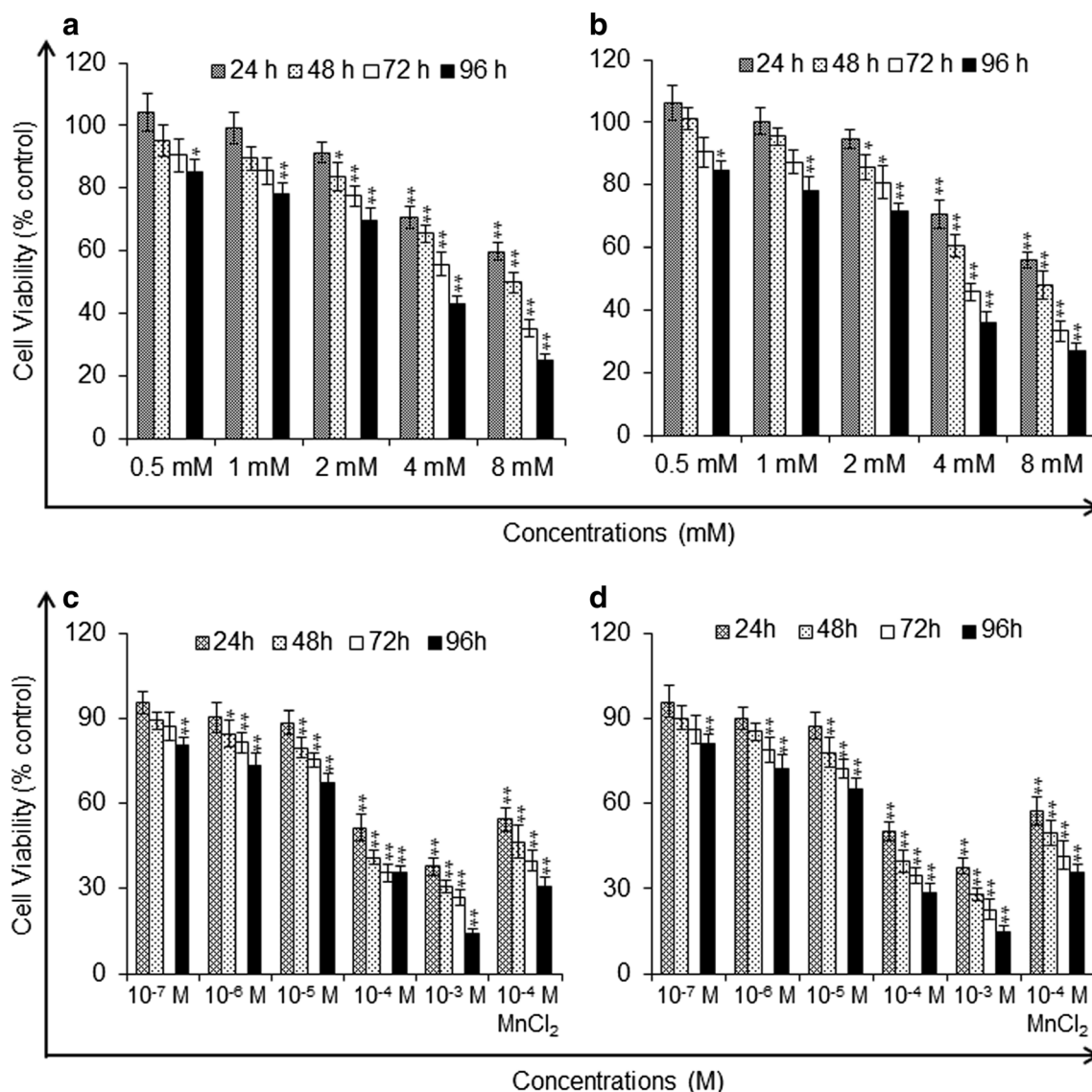


**Fig. 2** Identification of noncytotoxic doses of cyclophosphamide (CPA) and known neurotoxicant monocrotophos (MCP) in SH-SY5Y and U373-MG cell lines. Cells were exposed to CPA (0.5–8 mM) for 24–96 h in SH-SY5Y (a) and U373-MG cells (b) and MCP ( $10^{-7}$ – $10^{-3}$  M)

for 24–96 h in SH-SY5Y (c) and U373-MG cells (d). The percent cell viability was assessed using MTT assay. Values are given as mean  $\pm$  SE of the data obtained from three independent experiments. \* $p < 0.05$ , \*\* $p < 0.01$  in comparison to unexposed control

neuronal cells. However, the magnitude of expression was little bit lower than neural cells (Fig. 3a, b).

Neural cells responded significantly against cyclophosphamide (CPA; 2 mM) exposure for 3, 6, and 12 h by inducing the expression levels of CYP3A4 mRNA ( $5.69 \pm 0.76$ -,  $8.21 \pm 0.91$ -, and  $13.94 \pm 1.13$ -fold of control, respectively). Preexposure of CPA (12 h) provided an additive response to MCP-induced expressions of CYP3A4 mRNA in neural cells. The similar trend and magnitude of induction in the expression levels of CYP3A4 mRNA was also recorded in glial cells (Fig. 3c, d).

Unlike the transcriptional changes, the CYP regulator receptors (CAR and PXR) were significantly upregulated in both cells in time-dependent manner after the exposure of CPA. Preexposure of CPA (12 h) provided an additive response to MCP-induced expressions of mRNA of CAR and PXR in both neural and glial cells (Fig. 4a–d).

#### Docking Studies

In the present study, we explored the orientation and binding affinity (in terms of docking score and binding residues) of CPA and MCP toward the CAR and PXR, respectively



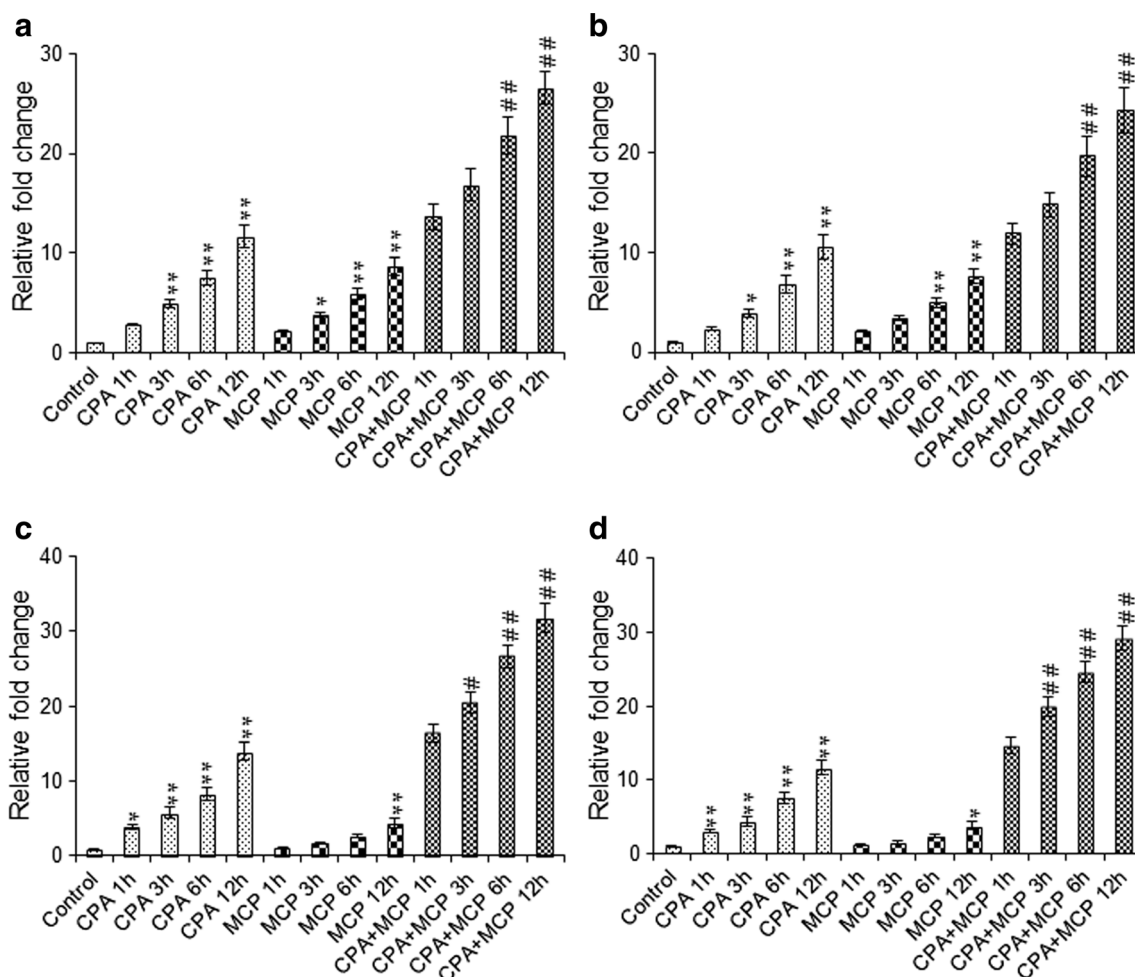


**Fig. 3** Real-time PCR analysis for transcriptional changes in CYP2C8 and CYP3A4 genes in SH-SY5Y and U373-MG cells. Fold changes in altered mRNA expression of CYP2C8 in SH-SY5Y (a) and U373-MG cells (b) following the exposure of CPA (1–12 h), MCP (1–12 h), and CPA (12 h) then MCP (1–12 h) groups. Fold changes in altered mRNA expression of CYP3A4 in SH-SY5Y (c) and U373-MG cells (d) following the exposure of CPA (1–12 h), MCP (1–12 h), and CPA

(12 h) then MCP (1–12 h) groups.  $\beta$ -Actin was used as endogenous control to normalize the data and xenobiotic exposure induced alterations in transcripts are expressed in fold changes (mean  $\pm$  SE) compared with unexposed controls. \* $p$  < 0.05 and \*\* $p$  < 0.01 in comparison to respective unexposed controls, while # $p$  < 0.05 and ## $p$  < 0.01 in comparison to CPA (12 h) exposure, respectively

(Table 1). Autodock results showed that the binding energy of CPA toward the CAR has high binding affinity (−5.35 kcal/mol, Fig. 5a) as compared to the docking score of MCP with CAR (−4.39 kcal/mol, Fig. 5b), docking score of CPA toward the PXR also has high binding affinity (−5.32 kcal/mol, Fig. 5d) as compared to the docking score of MCP with PXR (−4.69 kcal/mol, Fig. 5e). After that, we analyzed the binding affinity of MCP on already docked complex of CAR-CPA and PXR-CPA, where we scrutinized the combine synergistic effects of MCP and CPA on already exposed CAR and PXR receptors. The binding energy of MCP amplified toward the already exposed CAR with CPA from −4.39 to −5.34 kcal/mol (Fig. 5c). On other hand, MCP binding energy improved from −4.69 to −5.47 kcal/mol in case of PXR-CPA dock complex (Fig. 5f).

**Estimation of ROS Levels** The results of MCP ( $10^{-5}$  M) induced ROS generation are summarized in Fig. 6a. Cells showed significant ( $p$  < 0.01) responsiveness against MCP at each time point. The neural cells showed  $119.71 \pm 3.76$ ,  $135.42 \pm 4.77$ ,  $161.21 \pm 2.47$ , and  $183.34 \pm 6.11$ , and glial cells showed  $113.89 \pm 3.10$ ,  $127.63 \pm 5.27$ ,  $153.26 \pm 4.28$ , and  $179.14 \pm 6.48$  at 3, 6, 12, and 24 h, respectively, in comparison to control.

**Estimation of LPO Levels** Results of MCP-induced lipid peroxidation in neural and glial cells is presented in Fig. 6b. A time-dependent significant induction in LPO was observed for MCP ( $10^{-5}$  M) exposure, i.e.,  $103.49 \pm 3.01$ ,  $115.61 \pm 5.58$ ,  $129.77 \pm 3.59$ , and  $167.13 \pm 4.86$  % in neural cells and  $105.76 \pm 2.55$ ,  $113.56 \pm 4.23$ ,  $127.81 \pm 3.41$ , and  $159.36 \pm 4.69$  % in

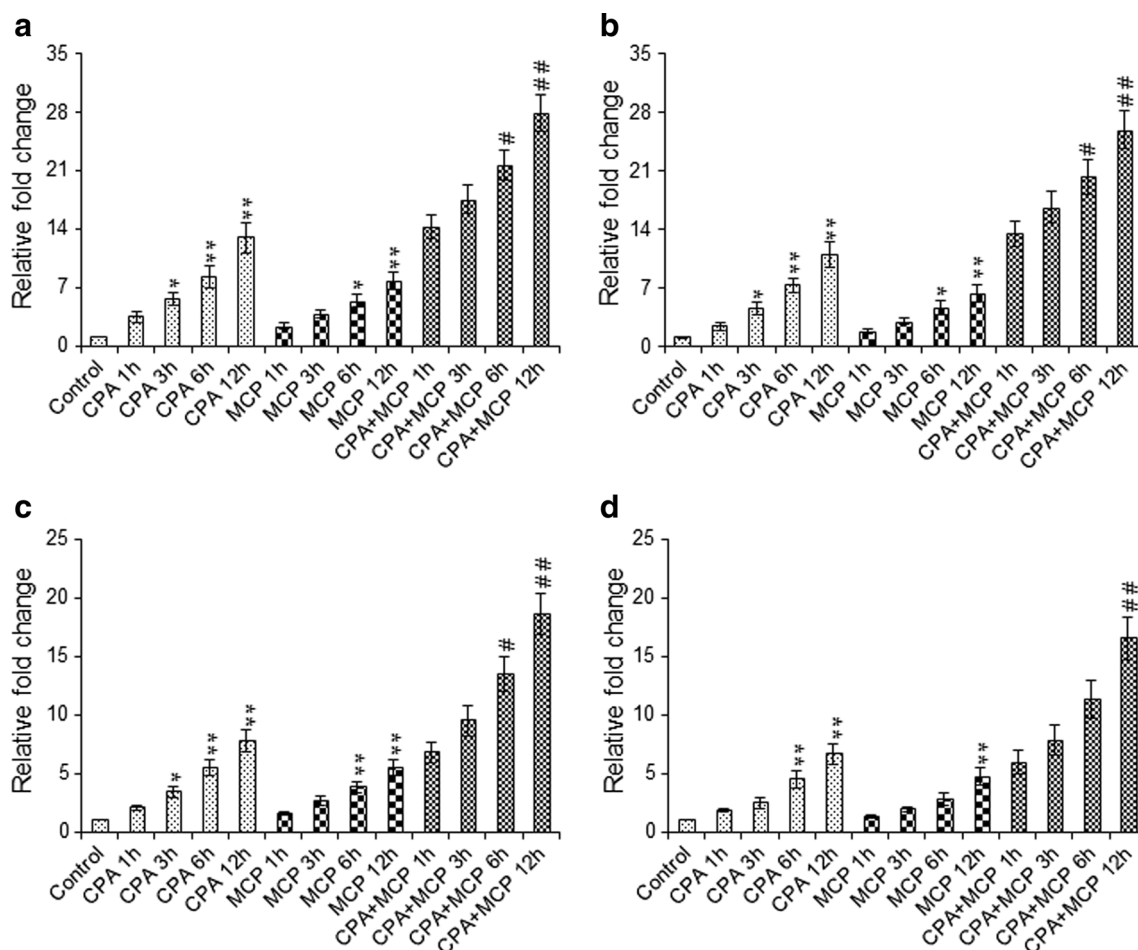


**Fig. 4** Real-time PCR analysis for transcriptional changes in CAR and PXR receptor genes in SH-SY5Y and U373-MG cells. Fold changes in altered mRNA expression of CAR in SH-SY5Y (a) and U373-MG cells (b) following the exposure of CPA (1–12 h), MCP (1–12 h), and CPA (12 h) then MCP (1–12 h) groups. Fold changes in altered mRNA expression of PXR in SH-SY5Y (c) and U373-MG cells (d) following the exposure of CPA (1–12 h), MCP (1–12 h), and CPA (12 h) then MCP

(1–12 h) groups.  $\beta$ -Actin was used as endogenous control to normalize the data and xenobiotic exposure induced alterations in transcripts are expressed in fold changes (mean  $\pm$  SE) compared with unexposed controls. \* $p < 0.05$  and \*\* $p < 0.01$  in comparison to respective unexposed controls, while # $p < 0.05$  and ## $p < 0.01$  in comparison to CPA (12 h) exposure, respectively

glial cells at 3, 6, 12, and 24 h, respectively, in comparison to control.

**Estimation of GSH Levels** Both the neural and glial cells exposed to MCP ( $10^{-5}$  M) were found to deplete the levels of GSH significantly at all the time points. The neural cells showed  $93.36 \pm 4.47$ ,  $77.41 \pm 3.16$ ,  $56.73 \pm 4.74$ , and  $34.96 \pm 3.73$  %, and the glial cells showed  $95.23 \pm 7.03$ ,  $83.18 \pm 4.89$ ,  $64.49 \pm 3.05$ , and  $47.69 \pm 2.22$  % at 3, 6, 12, and 24 h, respectively, in comparison to control (Fig. 6c).

**Estimation of Catalase Levels** Significant reduction in the activity of catalase was observed at  $10^{-5}$  M concentration of MCP, which was maximum at 24 h ( $37.29 \pm 2.53$  % in neural cells and  $41.88 \pm 5.38$  % in glial cells) followed by 12 h ( $61.31 \pm 3.67$  % in neural cells and  $67.35 \pm 4.51$  % in glial cells) and minimum at 3 h ( $96.22 \pm 4.42$  % in neural cells

and  $98.16 \pm 3.53$  % in glial cells) in the MCP-exposed cells (Fig. 6d).

**Transcriptional Changes in Apoptotic Genes** Apoptotic studies have been carried out in both neural and glial cells after the exposure of MCP ( $10^{-5}$  M). The significant upregulation of proapoptotic genes bax, p53, caspase-3, and caspase-9 and downregulation of antiapoptotic gene bcl2 have been recorded after the exposure of MCP in both cell types. The neural cells showed the upregulation of bax ( $1.55 \pm 0.08$ ,  $2.18 \pm 0.13$ ,  $2.95 \pm 0.10$ , and  $3.74 \pm 0.16$ ), p53 ( $1.84 \pm 0.08$ ,  $2.61 \pm 0.14$ ,  $4.25 \pm 0.18$ , and  $5.37 \pm 0.23$ ), caspase-3 ( $1.69 \pm 0.12$ ,  $2.57 \pm 0.08$ ,  $4.28 \pm 0.27$ , and  $6.72 \pm 0.20$ ), and caspase-9 ( $1.97 \pm 0.10$ ,  $4.19 \pm 0.15$ ,  $7.45 \pm 0.18$ , and  $9.28 \pm 0.21$ ), as well as the downregulation of bcl2 ( $0.91 \pm 0.06$ ,  $0.83 \pm 0.03$ ,  $0.61 \pm 0.03$ , and  $0.47 \pm 0.02$ ) at the exposure periods of 3, 6, 12, and 24 h, respectively, after the exposure of MCP. The trends were

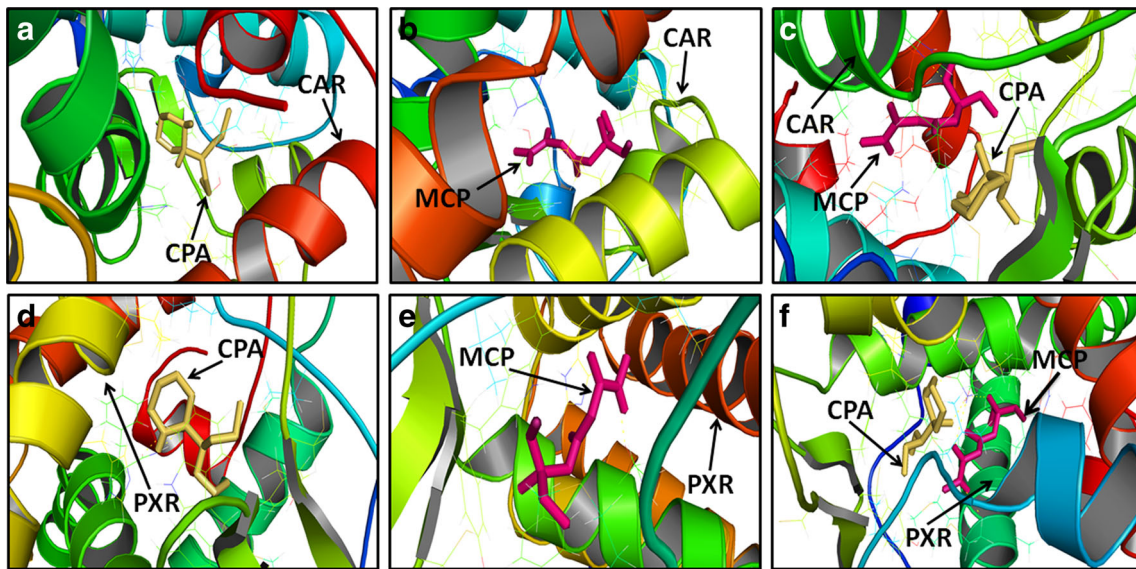


**Fig. 5** Crystal structure of receptors with docked ligands. **a** Cocrystallized structure of CAR and docked compound cyclophosphamide. **b** Cocrystallized structure of CAR and docked compound monocrotophos. **c** Cocrystallized structure of CAR and docked compound cyclophosphamide and monocrotophos. **d**

Cocrystallized structure of PXR and docked compound cyclophosphamide. **e** Cocrystallized structure of PXR and docked compound monocrotophos. **f** Cocrystallized structure of PXR and docked compound cyclophosphamide and monocrotophos

similar in the expression of bax, p53, caspase-3, caspase-9, and bcl2 in glial cells after the exposure of MCP at the same time points (Fig. 7 a–e).

**Translational Changes in Apoptotic Genes** The translational studies were carried out using Western blot analysis and have shown similar trends of expression of apoptotic genes as to that of transcription levels. Apoptotic studies have been carried out in both neural and glial cells after the exposure of MCP ( $10^{-5}$  M). The significant upregulation of proapoptotic genes bax, caspase-3, and p53 and downregulation of antiapoptotic gene bcl2 have been also recorded through Western blot after the exposure of MCP in both cell types. The neural cells showed the upregulation of bax ( $1.17 \pm 0.07$ ,  $1.25 \pm 0.10$ ,  $1.63 \pm 0.14$ , and  $1.99 \pm 0.09$ ), p53 ( $1.06 \pm 0.03$ ,  $1.46 \pm 0.06$ ,  $1.88 \pm 0.09$ , and  $2.33 \pm 0.12$ ), caspase-3 ( $1.38 \pm 0.11$ ,  $2.02 \pm 0.13$ ,  $2.67 \pm 0.16$ , and  $2.84 \pm 0.07$ ), and caspase-9 ( $1.96 \pm 0.12$ ,  $2.67 \pm 0.13$ ,  $3.31 \pm 0.16$ , and  $3.37 \pm 0.20$ ) as well as the downregulation of bcl2 ( $0.93 \pm 0.06$ ,  $0.79 \pm 0.08$ ,  $0.40 \pm 0.05$ , and  $0.37 \pm 0.03$ ) at the exposure periods of 3, 6, 12, and 24 h, respectively, after the exposure of MCP (Fig. 8a). The trends were similar in the expression of bax, p53, caspase-3, caspase-9, and bcl2 in glial cells after the exposure of MCP ( $10^{-5}$  M) at the same time points (Fig. 8b).

**Translocation of Bax and Cytochrome-c** The involvement of mitochondria-mediated apoptotic pathways in SH-SY5Y and U373-MG cells exposed to MCP ( $10^{-5}$  M) was confirmed by the translocation of Bax protein from cytosol to mitochondria and cytochrome-c protein from mitochondria to

cytoplasm using Western blot analysis. There was a significantly higher translocation of proteins between mitochondria and cytoplasm in cells exposed to MCP. The high purity of both cytosolic and mitochondrial fractions could be ascertained as there was no cross-contamination of the cytosol and mitochondria-specific proteins (Fig. 9a, b).

**Activity of Caspase-9 and Caspase-3** Highlights of MCP-induced alterations in the activity of caspase-9 and caspase-3 are shown in Fig. 10a, b, respectively. The activity of caspase-9 increased with increasing the exposure periods, i.e., 6, 12, and 24 h at  $10^{-5}$  M concentration of MCP. Interestingly, maximum induction in the activity of caspase-9 was recorded at 24 h of exposure, i.e.,  $156 \pm 2.89$  and  $147 \pm 1.73$  % in neural and glial cells, respectively (Fig. 10a). Caspase-3 activity was also found to be induced under the influence of MCP exposure in a time-dependent manner. However, maximum increase in activity of caspase-3 was recorded at 24 h of exposure of MCP followed by 3, 6, and 12 h, respectively (Fig. 10b). The increase in the activity of both caspase-9 and caspase-3 was statistically significant ( $p < 0.01$ ) when compared with unexposed control.

**MN Assay** MN assay was carried out to assess the accumulation of genetic damage in the cells. The cells were grown in DMEM/F-12 medium alone served as basal control and the other set of cells exposed to  $10^{-5}$  M concentration of MCP for different time periods were considered as treatment groups. The increase in the MN frequency was observed as compared to the growing of the cells in normal medium. We observed a

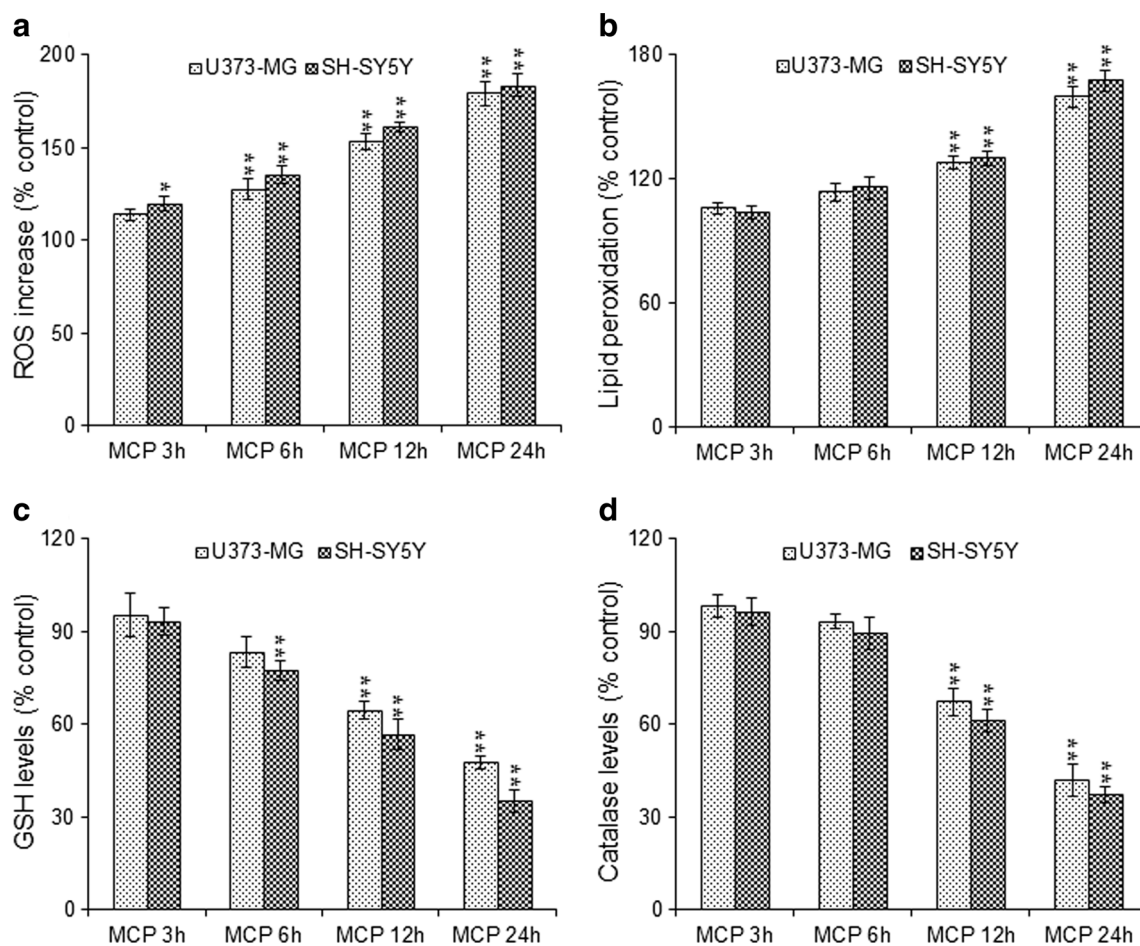


**Fig. 6** Oxidative stress study in SH-SY5Y and U373-MG cells. Percent change in ROS generation (a), change in levels of lipid peroxidation (b), GSH activity (c), and catalase activity (d) after the exposure of  $10^{-5}$  M concentration of MCP for 3, 6, 12, and 24 h time periods assessed by

microplate reader. Data represented are mean  $\pm$  SE of three identical experiments made in three replicates. \* $p < 0.05$  and \*\* $p < 0.01$  in comparison to respective unexposed controls

significant increase in the induction of MN following the exposure of cells to  $10^{-5}$  M of MCP. SH-SY5Y cells were showing  $12 \pm 1.15$ ,  $17 \pm 2.31$ , and  $23 \pm 3.46$  MN/1000 cells at 6, 12, and 24 h, respectively. Whereas, the U373-MG cells showed  $8 \pm 1.73$ ,  $13 \pm 1.73$ , and  $19 \pm 2.89$  MN/1000 cells for all time periods, i.e., 6–24 h (Fig. 11a).

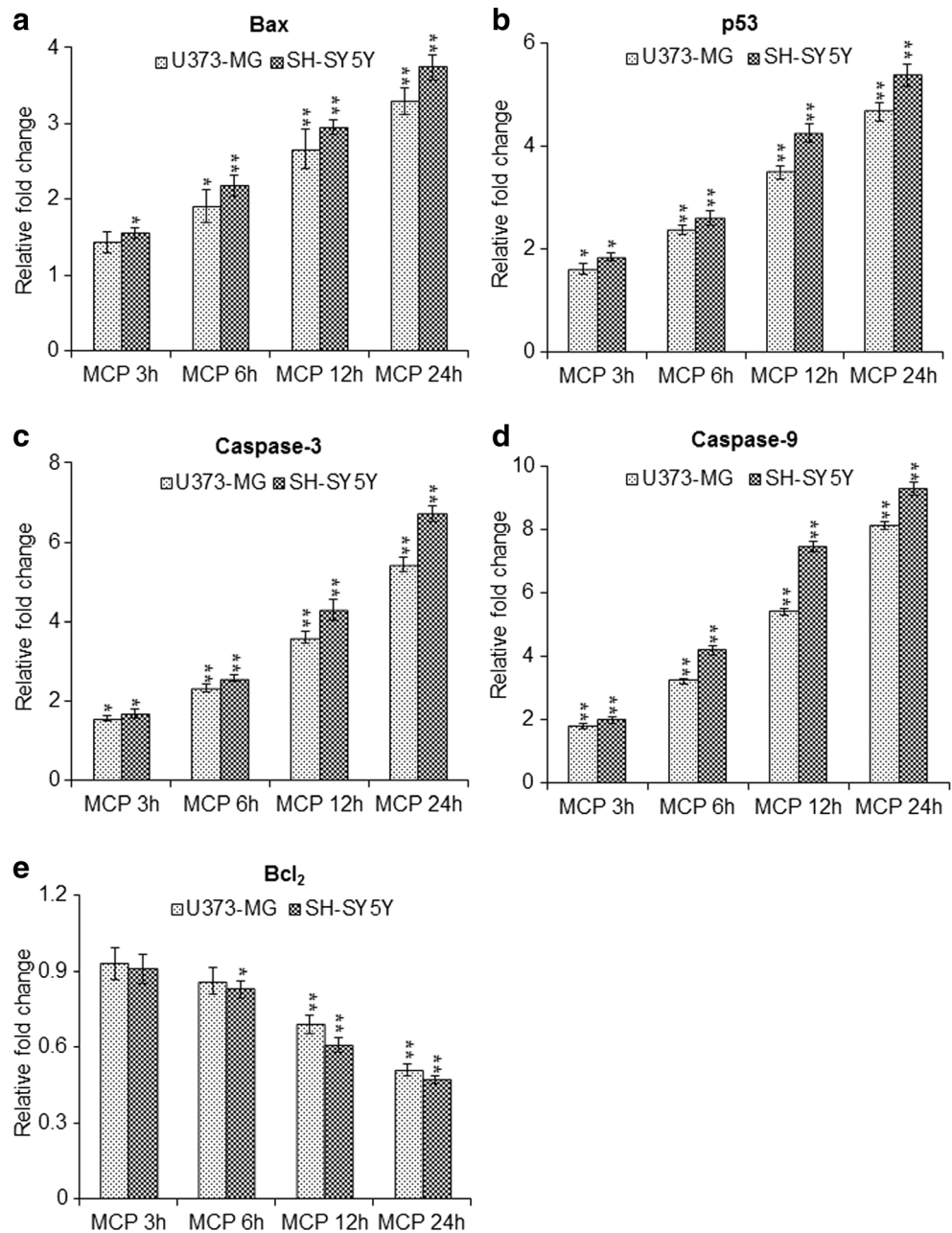
**CA Assay** The trends were similar as that to MN assay in both neural and glial cells. The most common aberrations were found of chromatid gaps and break type, followed by  $10^{-5}$  M concentration of MCP. The induction of CA in SH-SY5Y cells was  $9 \pm 1.15$ ,  $15 \pm 2.31$ , and  $24 \pm 1.73$  whereas in U373-MG cells  $6 \pm 1.73$ ,  $12 \pm 1.15$ , and  $21 \pm 2.31$  aberrations/100 in cells exposed to  $10^{-5}$  M for 6, 12, and 24 h, respectively (Fig. 11b).

## Discussion

The P450s have a critical role in the activation and deactivation of many toxic foreign chemicals, drugs, pesticides, and

other potentially toxic environmental compounds, as well as in the metabolism of cholesterol, bile acids, steroids, arachidonic acid, eicosanoids, vitamin D3, and retinoic acid. The presence of these proteins in both the brain and the blood-brain barrier (BBB) could be important for the production of biologically active compounds from centrally active drugs and environmental toxicants that cross the BBB. The endogenous substrates and the relative expression of specific forms of cytochrome P450 in specific areas of the brain are important to understand the effect of toxic substances in the brain [42]. Instead, CYPs appear to have specific functions in brain, e.g., regulation of the levels of endogenous GABA<sub>A</sub> receptor agonist's maintenance of brain cholesterol homeostasis and elimination of retinoids. The novel CYPs which catalyze these reactions have recently been characterized. They are abundantly expressed in the brain confirming what has been previously found, i.e., that the major hepatic, adrenal, and gonadal CYP isozymes contribute very little to the overall content of CYP in brain. Induction of these P450s by neuroactive drugs can alter steroid hormone signaling directly in drug target

**Fig. 7** Real-time PCR analysis for transcriptional changes in apoptotic genes in SH-SY5Y and U373-MG cells. Fold changes in altered mRNA expression of apoptotic genes in SH-SY5Y and U373-MG cells following the exposure of MCP (3–24 h).  $\beta$ -Actin was used as endogenous control to normalize the data and MCP induced alterations in transcripts are expressed in fold changes (mean  $\pm$  SE) compared with unexposed controls. \* $p < 0.05$  and \*\* $p < 0.01$  in comparison to respective unexposed controls

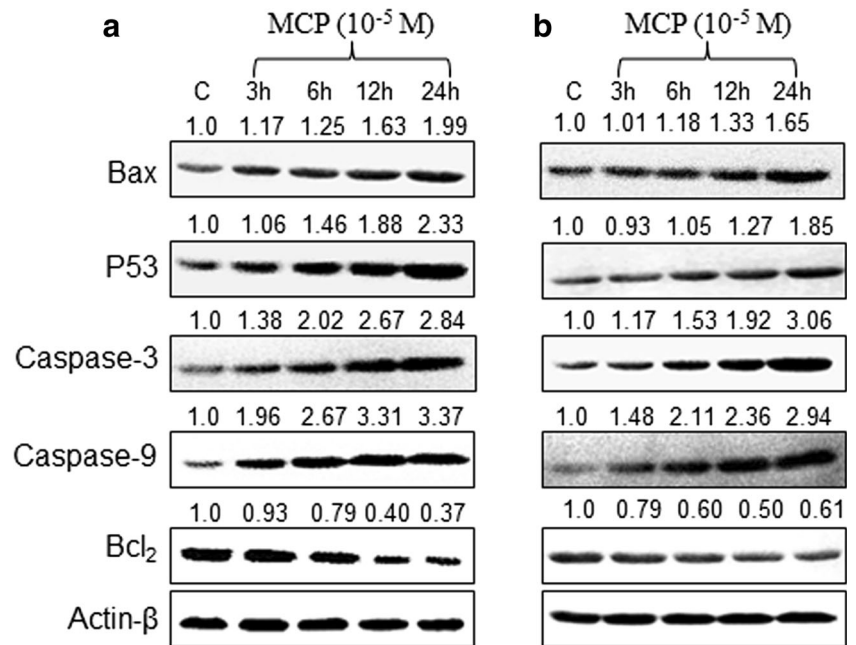


cells, which may cause clinically relevant side effects like reproductive disorders and sexual or mental dysfunction.

Neural and glial cells showed the expression and inducibility of CYP2C8 and CYP3A4 after the exposure of CPA and MCP. CPA induces significant expression of CYP2C8 and CYP3A4 but MCP alters the expression of CYP2C8 and CYP3A4 which could be indicative of their metabolism in these cells. Even though the magnitude of induction was not as high as we observed after the exposure of CPA, it reached to significant levels when the cells were exposed to a longer period of time. The expression of CYP2C8 increases as the

time period is increased, and it reached a maximum level at 12 h after the exposure of CPA in SH-SY5Y and U373-MG cells. In the brain, CYP2C8 mRNA is expressed at a higher level than other CYP2C mRNAs, and CYP2C8 mRNA is expressed at higher levels in brain than any other extra hepatic tissues tested. Low levels of CYP2C9 and 2C19 mRNAs were reported in the whole brain [43], where these enzymes could be implicated in the local metabolism of psychoactive drugs and xenobiotics as well as possibly in the regulation of the cerebral blood flow through production of EETs. mRNAs of CYP2C subfamily members such as CYP2C8 and 2C9 have

**Fig. 8** Western blot analysis for MCP induced translational changes in apoptotic gene proteins in SH-SY5Y and U373-MG cells. **a** Western blot analysis of expression of apoptotic gene proteins in SH-SY5Y cells following the exposure of MCP (3–24 h). **b** Western blot analysis of expression of apoptotic gene proteins in U373-MG cells following the exposure of MCP (3–24 h). The values obtained in unexposed cells were considered basal, i.e., relative quantification in expression at different point of various exposures was done comparing the values of unexposed controls.  $\beta$ -Actin was used as endogenous control to normalize the data

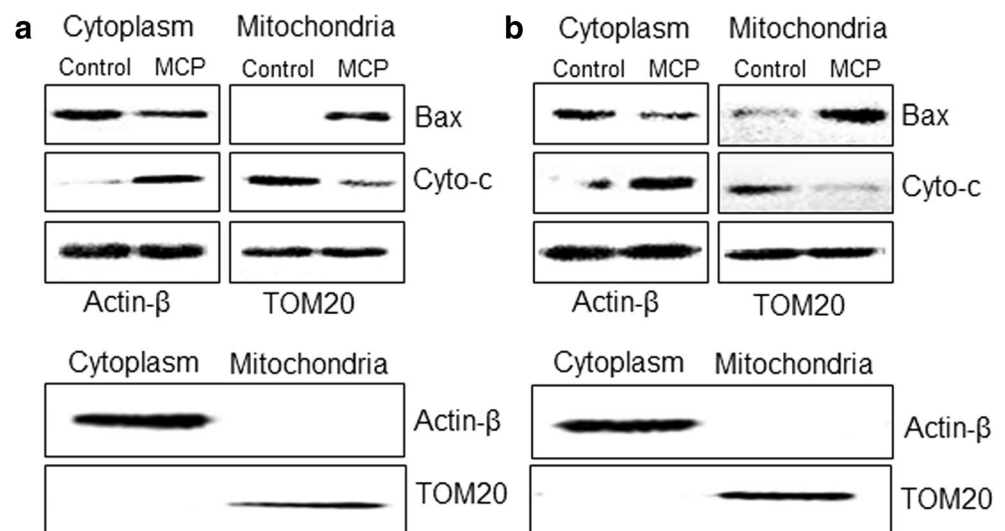


also been identified in human astrocytoma cells [44]. Cocaine treatment reduced mRNAs or proteins of CYP2C8 and 2C9 in human U373-MG astrocytoma cells, along with a simultaneous downregulation of CAR and GR, two nuclear receptors which could be involved in this reduction [44]. All three expressed CYP2C enzymes are inducible by ligands of the PXR/CAR, glucocorticoid (GR), and vitamin D (VDR) nuclear receptor pathways through different response elements in their 5'-flanking regions [45]. Our real-time data also showed a significant increase in the expression of CAR and PXR after the exposure of CPA. However, the genes show different relative inducibility, CYP2C8 is the most strongly inducible member, e.g., by statins [46]. Although distal PXR/CAR binding sites have been identified but the precise reason for the

high inducibility of CYP2C8 has not been elucidated. CYP2C8, an arachidonic acid epoxygenase [47], may have an endogenous function in the brain and regulates the modulation of cerebral vascular tone and blood flow in brain microvessels [48].

Both the SH-SY5Y and U373-MG cells showed significant expression of CYP3A4 after the exposure of CPA but MCP alone again failed to induce the significant expression of CYP3A4. MCP-induced alteration in the expression of CYPs showing additive responses in both neural and glial cells receiving a preexposure (12 h) of CPA. Such additive effects of MCP to the expression of CYPs studied in presensitized cells indicate the involvement of these CYPs in the metabolism of MCP. The findings also indicate that

**Fig. 9** Translocation study of cytoplasmic Bax protein to mitochondria and mitochondrial cytochrome-c protein to cytoplasm in SH-SY5Y and U373-MG cells: translocation of cytoplasmic Bax protein to mitochondria and mitochondrial cytochrome-c protein to cytoplasm in SH-SY5Y (a) and U373-MG (b) cells following the exposure of  $10^{-5}$  M concentration of MCP for 24 h. Lane 1, untreated control, and lane 2, cells exposed to  $10^{-5}$  M of MCP. TOM20 and  $\beta$ -actin were used to assess the purity of proteins isolated from mitochondria and cytoplasm, respectively



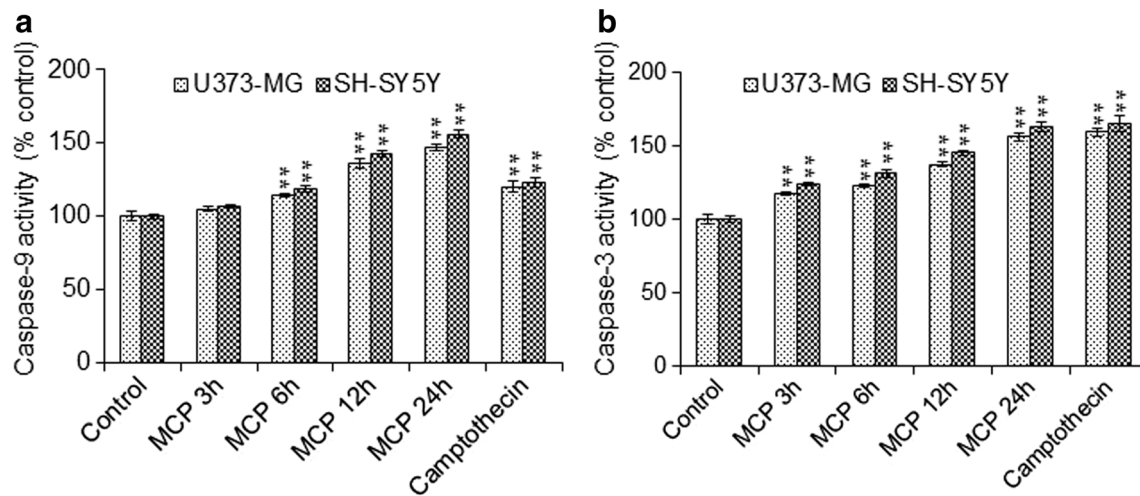


**Fig. 10** Induction in the activity of caspase-9 and caspase-3 in SH-SY5Y and U373-MG cells. **a** Induction in the activity of caspase-9 in SH-SY5Y and U373-MG cells exposed to MCP ( $10^{-5}$  M) for different time periods. \* $p < 0.05$ ; \*\* $p < 0.01$ . **b** Induction in the activity of caspase-3 in SH-

SY5Y and U373-MG cells exposed to MCP ( $10^{-5}$  M) for different time periods. Cells exposed with camptothecin (1  $\mu\text{g/mL}$ ) for 24 h as a positive control. \* $p < 0.05$ ; \*\* $p < 0.01$

nonsensitized cells did not have enough triggering signals to induce the expression like primary cultures of rat brain neural and glial cells [49] and in PC12 cells [31]. CYP3A4 also plays an important role in the metabolism of several endogenous substances, including testosterone, progesterone, androstenedione, and bile acids [50, 51]. CYP3A4 is the only human drug-metabolizing P450 that shows a significant sex difference; for instance women approximately express 1.5- to 2-fold more CYP3A4 than men do [52, 53]. The mechanism(s) behind the sex differences in expression is presumably transcriptional in nature and they may be related to the sex differences in plasma growth hormone profiles [54].

The minimum expression of CYP3A4 in astrocytes and limited drug metabolism capacity of glial cells have been

reported by Ghosh et al. [55] in human epileptic brain. This is in agreement with the study of Meyer et al. [7] showing that CYP3A4 is not expressed by glial cells, whereas other isoforms (e.g., CYP1A1, CYP2C) are present. They have shown glial expression of CYP3A4 only in a cavernous angiomas specimen whereas Gervasini et al. [14] had reported the expression of CYP3A4 in cultured brain tumor cells of astrocytic origin (glioblastoma or astrocytomas). The region- and cell-specific expression of CYPs in the brain may provide some insight into their functional significance and metabolic roles. For example, the high expression of CYP2B6 at the blood-brain interface may help to regulate the penetration of drugs and toxins into the brain [7]. Ghosh et al. [55] supports the expression of CYP3A4 at the BBB

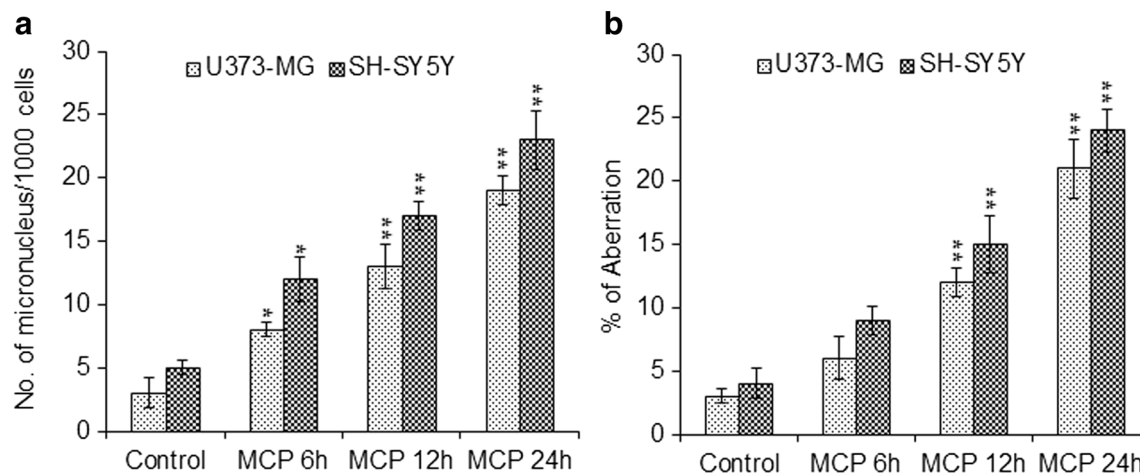


**Fig. 11** Genotoxicity/biosafety assessment of MCP ( $10^{-5}$  M) in SH-SY5Y and U373-MG cells. Micronuclei (MN) induction in SH-SY5Y and U373-MG cells exposed to  $10^{-5}$  M concentration of MCP for different time periods (**a**). Micronuclei were calculated by scoring a minimum of 1000 cells. Chromosomal aberration (CA) in SH-SY5Y

and U373-MG cells exposed to  $10^{-5}$  M concentration of MCP for different time periods (**b**). Values are given as mean  $\pm$  standard error of the data obtained from three independent experiments and each experiment contained at least three replicates. \* $p < 0.05$ , significant

endothelial and neuronal cells of drug-resistant epileptic subjects. CYP3A4, along with MDR1, may affect the brain biotransformation of drugs and be involved in mechanism of cell survival in the diseased brain.

CYP3A4 oxidizes a broad spectrum of antiepileptic drugs (AEDs), allowing for detoxification/elimination processes. This clearance process is potentially relevant since AEDs may cause an excess of undesirable and sometimes permanent neurologic effects including dyskinesia, myoclonus, and tremor [56, 57]. The upstream factor PXR has also been reported to play an important role in protection against DNA damage [58]. The PXR activation induces cerebellar CYP expression, thereby attenuating neural injury [59]. This suggests that a pharmacologic induction of CYP3A4 in brain cells may have a profound effect on neural survival. On the other hand, the coadministration of any CYP inhibitors may aggravate AED neurotoxicity. One report indicates that the administration of a CYP3A4 inhibitor (e.g., ritonavir and efavirenz) resulted in increased CBZ-induced ataxia in patients [60].

Monocrotophos is one of the most widely used OP pesticides throughout the world. It is classified as extremely hazardous pesticide in India. The effect of MCP on cellular DNA and its potential to generate oxidative stress was examined in neural and glial cells. In the present investigations, the MCP-induced increase in expression levels of CYP2C8 and CYP3A4 that were not as high as those levels induced by CPA. MCP is documented as a potent developmental neurotoxicant which inhibits acetylcholine mediated neurotransmission in the brain [61]. Because of high lipid contents, brain cells are highly vulnerable to xenobiotics-induced oxidative stress prominent to high oxygen consumption and low levels of glutathione content [62, 63]. Oxygen free radicals and hydroperoxides collectively termed as ROS cause oxidative damage to biological membranes and macromolecules [64]. Oxidative stress induced by OP intoxication is associated with elevated lipid peroxidation and decreased antioxidant defense [61].

ROS generation is considered to be one of the strategic signals for oxidative stress-induced apoptosis [65]. In this study, significant ( $p < 0.01$ ) generation of ROS, LPO, and increased ratio of GSH were observed in both neural and glial cells exposed to selected dose of MCP. Reduced glutathione is the principal antioxidant molecule in scavenging and detoxification of free radicals and preventing oxidative damage [66]. Oxidative damage is also suppressed by the activities of key antioxidant enzymes especially SOD, glutathione peroxidase, and catalase. The generation of ROS has been reported to decrease the GSH and enhance the LPO production, which leads to apoptosis in a variety of cells such as astrocytes [67], PC12 cells [68, 69], and tissues of rat brain [70, 71]. Organochlorine pesticides are also reported to induce ROS generation, which subsequently

leads to apoptosis and cell death in mice [72], blood mononuclear cells [73], and mouse macrophage cell lines [74]. Thus, ROS generation in the present study may be a mediator for MCP-induced apoptosis in neural and glial cells. Organophosphates pesticides including paraoxon, parathion, PSP, TOTP, and TPPi induced apoptosis that is associated with nuclear condensation, budding, caspase-3 activation, and DNA fragmentations in SHY-SY-5Y, a human neuroblastoma cell line [75]. We observed that MCP significantly upregulated in the expression of caspase-3, caspase-9, Bax, p53, and downregulated Bcl<sub>2</sub>. Upregulation of nuclear p53 protein is known to play an important role in minimizing DNA damage by inducing transcriptional reprogramming, which finally leads to controlled cell death [76, 77].

MCP has been widely investigated for its genotoxic and mutagenic potential. MN formation is an indication of fragmentation in chromosomes and that fragment is not incorporated into daughter nuclei during mitosis. Although CA is referred as a missing, extra, or an irregular portion of chromosomal deoxyribonucleic acid, this is not integrated into daughter nuclei. Xenobiotic exposures have been demonstrated to form an atypical number of chromosomes or a structural abnormality in one or more chromosomes due to MN and/or CA. Our findings revealed that the  $10^{-5}$  M concentration of MCP significantly induces the MN and CA in both the neural and glial cells. It is also reported that MCP induces lethal mutations in male germ-line cells and somatic cells of *Drosophila melanogaster* [78]. The genotoxicity and mutagenicity tests of MCP were positive when they were evaluated by in vivo test system employing micronucleus bioassay in chicken, using the chromosome aberration (CA) assay in bone marrow cells, and the micronucleus test in both bone marrow and peripheral blood erythrocytes (Ames test and Salmonella lactam test) [79, 80]. Zahran et al. [81] reported high incidence of structural and numerical chromosomal aberrations in somatic and germ cells of male as well as liver and embryos of pregnant mice. The mitotic indexes, content of protein, RNA, DNA, and cholinesterase activity were reduced while an increase in the activity of gamma glutamyl transferase was observed following MCP exposure in mice.

We can conclude that the constitutive expression of CYP2C8 and CYP3A4 in cultured human neural (SH-SY5Y) and glial (U373-MG) may possibly be associated with the endogenous physiology of the brain. The responsiveness of both cell types against MCP exposure was enhanced due to a presensitization with CPA. In silico studies have suggested that binding energy of CPA toward the CAR is more than MCP with CAR. In the same way, the binding energy of CPA toward CAR is more than MCP with PXR. However, the binding affinity of MCP on already docked complex of CAR-CPA and PXR-CPA, where we scrutinized the combine



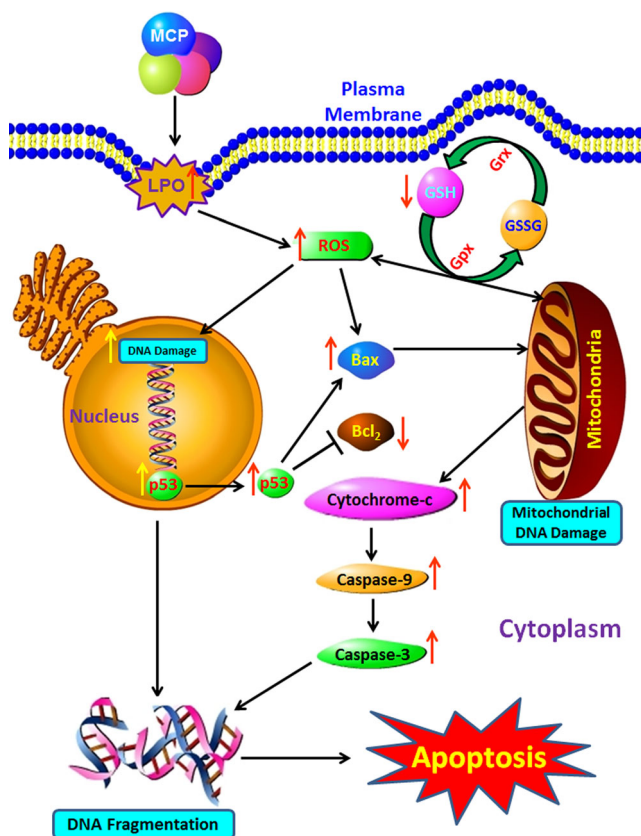


**Fig. 12** Schematic flow diagram to represent apoptotic pathway involved in human brain neuronal and glial cells exposed to MCP

additive effects of MCP and CPA on already exposed CAR and PXR receptors. Understanding the functional significance of brain CYPs may be valuable in developing more effective approaches to treat and prevent CNS diseases. However, the application of brain CYP metabolism to improve health care and drug development requires advancement in key areas. First, the molecular mechanisms regulating the region- and cell-specific expression of CYPs in the brain, and the impact of inducers and inhibitors should be better understood. Second, the impact of various brain CYP isoforms on drug/toxin sensitivity and response needs further investigation. Exposure of MCP causes increase in ROS which initiates oxidative damage. The increased ROS levels upregulate p53 and diminish Bcl2 protein, leading to a deteriorated ratio of Bcl-2/Bax. The alteration in Bcl2/Bax ratio results in the release of cytochrome-c. Finally, the release of cytochrome-c activates caspase-9 and subsequently triggers the caspase-3 cascade leading to apoptosis in U373-MG and SH-SY5Y cells (Fig. 12).

**Acknowledgments** This work was carried out with the support of a grant from the Next-Generation BioGreen 21 Program (Project No. PJ011101) and a grant for FTA issues (Project No. PJ01017003) of Rural Development Administration, Republic of Korea.

## Compliance with Ethical Standards

**Conflict of Interest** The authors of this manuscript have no conflict of interest among them or anybody else regarding the scientific contents, financial matters, or otherwise.

## References

- Korkina L, Scordo MG, Deeva I, Cesareo E, De Luca C (2009) The chemical defensive system in the pathobiology of idiopathic environment-associated diseases. *Curr Drug Metab* 10:914–931
- Conde-Vancells J, Gonzalez E, Lu SC, Mato JM, Falcon-Perez JM (2010) Overview of extra cellular microvesicles in drug metabolism. *Expert Opin Drug Metab Toxicol* 6:543–554
- Toselli F, de Waziers I, Dutheil M, Vincent M, Wilce PA, Dodd PR, Beaune P, Lorient MA et al (2015) Gene expression profiling of cytochromes P450, ABC transporters and their principal transcription factors in the amygdala and prefrontal cortex of alcoholics, smokers and drug-free controls by qRT-PCR. *Xenobiotica* 45: 1129–1137
- Singh AK, Kashyap MP, Jahan S, Kumar V, Tripathi VK, Siddiqui MA, Yadav S, Khanna VK et al (2012) Expression and inducibility of cytochrome P450s (CYP1A1, 2B6, 2E1, 3A4) in human cord blood CD34(+) stem cell-derived differentiating neuronal cells. *Toxicol Sci* 129:392–410
- Tripathi VK, Kumar V, Singh AK, Kashyap MP, Jahan S, Pandey A, Alam S, Khan F et al (2014) Monocrotophos induces the expression and activity of xenobiotic metabolizing enzymes in pre-sensitized cultured human brain cells. *PLoS One* 9:e91946
- Miksys S, Tyndale RF (2006) Nicotine induces brain CYP enzymes: relevance to Parkinson's disease. *J Neural Transm Suppl* 70:177–180
- Meyer RP, Gehlhaus M, Knoth R, Volk B (2007) Expression and function of cytochrome p450 in brain drug metabolism. *Curr Drug Metab* 8:297–306
- Delozier TC, Kissling GE, Coulter SJ, Dai D, Foley JF, Bradbury JA, Murphy E, Steenbergen C et al (2007) Detection of human CYP2C8, CYP2C9, and CYP2J2 in cardiovascular tissues. *Drug Metab Dispos* 35:682–688
- Zanger UM, Turpeinen M, Klein K, Schwab M (2008) Functional pharmacogenetics/genomics of human cytochromes P450 involved in drug biotransformation. *Anal Bioanal Chem* 392:1093–1108
- Goldstein JA (2001) Clinical relevance of genetic polymorphisms in the human CYP2C subfamily. *Br J Clin Pharmacol* 52:349–355
- Marill J, Cresteil T, Lanotte M, Chabot GG (2000) Identification of human cytochrome P450s involved in the formation of all-trans-retinoic acid principal metabolites. *Mol Pharmacol* 58:1341–1348
- Fleming I, Michaelis UR, Bredenkötter D, Fisslthaler B, Dehghani F, Brandes RP, Busse R (2001) Endothelium-derived hyperpolarizing factor synthase (Cytochrome P450 2C9) is a functionally significant source of reactive oxygen species in coronary arteries. *Circ Res* 88:44–51
- Bu HZ (2006) A literature review of enzyme kinetic parameters for CYP3A4-mediated metabolic reactions of 113 drugs in human liver microsomes: structure-kinetics relationship assessment. *Curr Drug Metab* 7:231–249
- Gervasini G, Carrillo JA, Benitez J (2004) Potential role of cerebral cytochrome P450 in clinical pharmacokinetics: modulation by endogenous compounds. *Clin Pharmacokinet* 43:693–706
- Hendrychova T, Anzenbacherová E, Hudeček J, Skopalík J, Lange R, Hildebrandt P, Otyepka M, Anzenbacher P (2011) Flexibility of

- human cytochrome P450 enzymes: molecular dynamics and spectroscopy reveal important function-related variations. *Biochim Biophys Acta* 1814:58–68
16. Wang RW, Newton DJ, Scheri TD, Lu AY (1997) Human cytochrome P450 3A4-catalyzed testosterone 6 beta-hydroxylation and erythromycin N-demethylation. Competition during catalysis. *Drug Metab Dispos* 25:502–507
  17. Lee AJ, Cai MX, Thomas PE, Conney AH, Zhu BT (2003) Characterization of the oxidative metabolites of 17beta-estradiol and estrone formed by 15 selectively expressed human cytochrome p450 isoforms. *Endocrinology* 144:3382–3398
  18. McEwen BS (1994) How do sex and stress hormones affect nerve cells? *Ann N Y Acad Sci* 743:1–16
  19. Munetsuna E, Hojo Y, Hattori M, Ishii H, Kawato S, Ishida A, Kominami SA, Yamazaki T (2009) Retinoic acid stimulates 17beta-estradiol and testosterone synthesis in rat hippocampal slice cultures. *Endocrinology* 150:4260–4269
  20. Kwong TC (2002) Organophosphate pesticides: biochemistry and clinical toxicology. *Ther Drug Monit* 24:144–149
  21. Kossmann S, Magner-Krezel Z, Sobieraj R, Szwed Z (1997) The assessment of nephrotoxic effect of organophosphorous pesticides based on the determination of the activity of some selected enzymes in urine. *Przegl Lek* 54:707–711
  22. Rawlings NC, Cook SJ, Waldbillig D (1998) Effects of the pesticides carbofuran, chlorpyrifos, dimethoate, lindane, triallate, trifluralin, 2,4-D, and pentachlorophenol on the metabolic endocrine and reproductive endocrine system in ewes. *J Toxicol Environ Health A* 54:21–36
  23. Gomes J, Dawodu AH, Lloyd O, Revitt DM, Anilal SV (1999) Hepatic injury and disturbed amino acid metabolism in mice following prolonged exposure to organophosphorus pesticides. *Hum Exp Toxicol* 18:33–37
  24. McDaniel KL, Moser VC (2004) Differential profiles of cholinesterase inhibition and neurobehavioral effects in rats exposed to fenamiphos or profenofos. *Neurotoxicol Teratol* 26:407–415
  25. Tiwari MN, Singh AK, Ahmad I, Upadhyay G, Singh D, Patel DK, Singh C, Prakash O et al (2010) Effects of cypermethrin on monoamine transporters, xenobiotic metabolizing enzymes and lipid peroxidation in the rat nigrostriatal system. *Free Radic Res* 44:1416–1424
  26. Tiwari MN, Singh AK, Agrawal S, Gupta SP, Jyoti A, Shanker R, Prakash O, Singh MP (2012) Cypermethrin alters the expression profile of mRNAs in the adult rat striatum: a putative mechanism of postnatal pre-exposure followed by adulthood re-exposure-enhanced neurodegeneration. *Neurotox Res* 22:321–334
  27. Ranjbar A, Pasalar P, Abdollahi M (2002) Induction of oxidative stress and acetylcholinesterase inhibition in organophosphorous pesticide manufacturing workers. *Hum Exp Toxicol* 21:179–182
  28. Junior HV, de França Fonteles MM, Mendes de Freitas R (2009) Acute seizure activity promotes lipid peroxidation, increased nitrite levels and adaptive pathways against oxidative stress in the frontal cortex and striatum. *Oxid Med Cell Longev* 2:130–137
  29. Masoud A, Kiran R, Sandhir R (2009) Impaired mitochondrial functions in organophosphate induced delayed neuropathy in rats. *Cell Mol Neurobiol* 29:1245–1255
  30. Kashyap MP, Singh AK, Siddiqui MA, Kumar V, Tripathi VK, Khanna VK, Yadav S, Jain SK et al (2010) Caspase cascade regulated mitochondria mediated apoptosis in monocrotophos exposed PC12 cells. *Chem Res Toxicol* 23:1663–1672
  31. Kashyap MP, Singh AK, Kumar V, Tripathi VK, Srivastava RK, Agrawal M, Khanna VK, Yadav S et al (2011) Monocrotophos induced apoptosis in PC12 cells: role of xenobiotic metabolizing cytochrome P450s. *PLoS One* 6:e17757
  32. Morris GM, Goodsell DS, Huey R, Olson AJ (1996) Distributed automated docking of flexible ligands to proteins: parallel applications of AutoDock 2.4. *J Comput Aided Mol Des* 10:293–304
  33. Pettersen EF, Goddard TD, Huang CC, Couch GS, Greenblatt DM, Meng EC, Ferrin TE (2004) UCSF Chimera—a visualization system for exploratory research and analysis. *J Comput Chem* 25:1605–1612
  34. Wang J, Wang W, Kollman PA, Case DA (2006) Automatic atom type and bond type perception in molecular mechanical calculations. *J Mol Graph Model* 25:247–260
  35. Wang J, Wolf RM, Caldwell JW, Kollman PA, Case DA (2004) Development and testing of a general amber force field. *J Comput Chem* 25:1157–1174
  36. Morris GM, Goodsell DS, Halliday RS, Huey R, Hart WE, Belew RK, Olson AJ (1998) Automated docking using a Lamarckian genetic algorithm and an empirical binding free energy function. *J Comput Chem* 19:1639–1662
  37. Rarey M, Kramer B, Lengauer T, Klebe G (1996) A fast flexible docking method using an incremental construction algorithm. *J Mol Biol* 261:470–489
  38. Goodsell DS, Morris GM, Olson AJ (1996) Automated docking of flexible ligands: applications of AutoDock. *J Mol Recognit* 9:1–5
  39. Schagger H (2006) Tricine-SDS-PAGE. *Nat Protoc* 1:16–22
  40. Siddiqui MA, Kashyap MP, Kumar V, Al-Khedhairy AA, Musarrat J, Pant AB (2010) Protective potential of trans-resveratrol against 4-hydroxynonenal induced damage in PC12 cells. *Toxicol In Vitro* 24:1592–1598
  41. Srivastava RK, Lohani M, Pant AB, Rahman Q (2010) Cytogenotoxicity of amphibole asbestos fibers in cultured human lung epithelial cell line: role of surface iron. *Toxicol Ind Health* 26:575–582
  42. Hedlund E, Gustafsson JA, Warner M (2001) Cytochrome P450 in the brain; a review. *Curr Drug Metab* 2:245–263
  43. McFayden MC, Melvin WT, Murray GI (1998) Regional distribution of individual forms of cytochrome P450 mRNA in normal adult human brain. *Biochem Pharmacol* 55:825–830
  44. Malaplate-Armand C, Ferrari L, Masson C, Visvikis-Siest S, Lambert H, Batt AM (2005) Down-regulation of astroglial CYP2C, glucocorticoid receptor and constitutive androstane receptor genes in response to cocaine in human U373 MG astrocytoma cells. *Toxicol Lett* 159:203–211
  45. Chen Y, Goldstein JA (2009) The transcriptional regulation of the human CYP2C genes. *Curr Drug Metab* 10:567–578
  46. Feidt DM, Klein K, Hofmann U, Riedmaier S, Knobloch D, Thasler WE, Weiss TS, Schwab M et al (2010) Profiling induction of cytochrome p450 enzyme activity by statins using a new liquid chromatography-tandem mass spectrometry cocktail assay in human hepatocytes. *Drug Metab Dispos* 38:1589–1597
  47. Zeldin DC, DuBois RN, Falck JR, Capdevila JH (1995) Molecular cloning, expression and characterization of an endogenous human cytochrome P450 arachidonic acid epoxygenase isoform. *Arch Biochem Biophys* 322:76–86
  48. Gebremedhin D, Ma YH, Falck JR, Roman RJ, VanRollins M, Harder DR (1992) Mechanism of action of cerebral epoxyeicosatrienoic acids on cerebral arterial smooth muscle. *Am J Physiol* 263:H519–H525
  49. Kapoor N, Pant AB, Dhawan A, Dwivedi UN, Seth PK, Parmar D (2007) Differences in the expression and inducibility of cytochrome P450 2B isoenzymes in cultured rat brain neuronal and glial cells. *Mol Cell Biochem* 305:199–207
  50. Yamazaki H, Shimada T (1997) Progesterone and testosterone hydroxylation by cytochromes P450 2C19, 2C9, and 3A4 in human liver microsomes. *Arch Biochem Biophys* 346:161–169
  51. Pikuleva IA (2006) Cytochrome P450s and cholesterol homeostasis. *Pharmacol Ther* 112:761–773
  52. Wolbold R, Klein K, Burk O, Nüssler AK, Neuhaus P, Eichelbaum M, Schwab M, Zanger UM (2003) Sex is a major determinant of CYP3A4 expression in human liver. *Hepatology* 38:978–988

53. Cotreau MM, von Moltke LL, Greenblatt DJ (2005) The influence of age and sex on the clearance of cytochrome P450 3A substrates. *Clin Pharmacokinet* 44:33–60
54. Waxman DJ, O'Connor C (2006) Growth hormone regulation of sex-dependent liver gene expression. *Mol Endocrinol* 20:2613–2629
55. Ghosh C, Marchi N, Desai NK, Puvenna V, Hossain M, Gonzalez-Martinez J, Alexopoulos AV, Janigro D (2011) Cellular localization and functional significance of CYP3A4 in the human epileptic brain. *Epilepsia* 52:562–571
56. Zaccara G, Cincotta M, Borgheresi A, Balestrieri F (2004) Adverse motor effects induced by antiepileptic drugs. *Epileptic Disord* 6: 153–168
57. Schmidt D (2009) Drug treatment of epilepsy: options and limitations. *Epilepsy Behav* 15:56–65
58. Naspinski C, Gu X, Zhou GD, Mertens-Talcott SU, Donnelly KC, Tian Y (2008) Pregnane X receptor protects HepG2 cells from BaP-induced DNA damage. *Toxicol Sci* 104:67–73
59. Langmade SJ, Gale SE, Frolov A, Mohri I, Suzuki K, Mellon SH, Walkley SU, Covey DF et al (2006) Pregnane X receptor (PXR) activation: a mechanism for neuroprotection in a mouse model of Niemann-Pick C disease. *Proc Natl Acad Sci U S A* 103:13807–13812
60. Burman W, Orr L (2000) Carbamazepine toxicity after starting combination antiretroviral therapy including ritonavir and efavirenz. *AIDS* 14:2793–2804
61. Kazi AI, Oommen A (2012) Monocrotophos induced oxidative damage associates with severe acetylcholinesterase inhibition in rat brain. *Neurotoxicology* 33:156–161
62. Aschner M, Allen JW, Kimelberg HK, LoPachin RM, Streit WJ (1999) Glial cells in neurotoxicity development. *Annu Rev Pharmacol Toxicol* 39:151–173
63. Rossi DJ, Brady JD, Mohr C (2007) Astrocyte metabolism and signaling during brain ischemia. *Nat Neurosci* 10:1377–1386
64. Kehrer JP (1993) Free radicals as mediators of tissue injury and disease. *Crit Rev Toxicol* 23:21–48
65. Kroemer G, Galluzzi L, Brenner C (2007) Mitochondrial membrane permeabilization in cell death. *Physiol Rev* 87:99–163
66. Cnubben NH, Rietjens IM, Wortelboer H, van Zanden J, van Bladeren PJ (2001) The interplay of glutathione-related processes in antioxidant defense. *Environ Toxicol Pharmacol* 10:141–152
67. Zhang J, Hu J, Ding JH, Yao HH, Hu G (2005) 6-Hydroxydopamine-induced glutathione alteration occurs via glutathione enzyme system in primary cultured astrocytes. *Acta Pharmacol Sin* 26:799–805
68. Kumar V, Tripathi VK, Jahan S, Agrawal M, Pandey A, Khanna VK, Pant AB (2015) Lead Intoxication Synergies of the Ethanol-Induced Toxic Responses in Neuronal Cells–PC12. *Mol Neurobiol* 52:1504–1520
69. Kumar V, Gupta AK, Shukla RK, Tripathi VK, Jahan S, Pandey A, Srivastava A, Agrawal M et al (2015) Molecular Mechanism of Switching of TrkA/p75(NTR) Signaling in Monocrotophos Induced Neurotoxicity. *Sci Rep* 5:14038
70. Slotkin TA, Seidler FJ (2007) Comparative developmental neurotoxicity of organophosphates in vivo: transcriptional responses of pathways for brain cell development, cell signaling, cytotoxicity and neurotransmitter systems. *Brain Res Bull* 72:232–274
71. Gonzalez-Santiago L, Suárez Y, Zarich N, Muñoz-Alonso MJ, Cuadrado A, Martínez T, Goya L, Iradi A et al (2006) Aclidin induces JNK-dependent apoptosis in human breast cancer cells via alteration of glutathione homeostasis, Rac1 GTPase activation, and MKP-1 phosphatase downregulation. *Cell Death Differ* 13: 1968–1981
72. Sun F, Anantharam V, Latchoumycandane C, Kanthasamy A, Kanthasamy AG (2005) Dieldrin induces ubiquitin-proteasome dysfunction in alpha-synuclein overexpressing dopaminergic neuronal cells and enhances susceptibility to apoptotic cell death. *J Pharmacol Exp Ther* 315:69–79
73. Perez-Maldonado IN, Herrera C, Batres LE, González-Amaro R, Diaz-Barriga F, Yáñez L (2005) DDT-induced oxidative damage in human blood mononuclear cells. *Environ Res* 98:177–184
74. Zhao M, Zhang Y, Wang C, Fu Z, Liu W, Gan J (2009) Induction of macrophage apoptosis by an organochlorine insecticide acetofenatate. *Chem Res Toxicol* 22:504–510
75. Carlson K, Jortner BS, Ehrlich M (2000) Organophosphorus compound-induced apoptosis in SH-SY5Y human neuroblastoma cells. *Toxicol Appl Pharmacol* 168:102–113
76. Bunz F, Dutriaux A, Lengauer C, Waldman T, Zhou S, Brown JP, Sedivy JM, Kinzler KW et al (1998) Requirement for p53 and p21 to sustain G2 arrest after DNA damage. *Science* 282:1497–1501
77. Cui Q, Yu JH, Wu JN, Tashiro S, Onodera S, Minami M, Ikejima T (2007) P53-mediated cell cycle arrest and apoptosis through a caspase-3-independent, but caspase-9-dependent pathway in oridonin-treated MCF-7 human breast cancer cells. *Acta Pharmacol Sin* 28:1057–1066
78. Tripathy NK, Patnaik KK (1992) Studies on the genotoxicity of monocrotophos in somatic and germ-like cells of *Drosophila*. *Mutat Res* 278:23–29
79. Bhunya SP, Jena GB (1993) Studies on the genotoxicity of monocrotophos, an organophosphate insecticide, in the chick in vivo test system. *Mutat Res* 292:231–239
80. Hour TC, Chen L, Lin JK (1998) Comparative investigation on the mutagenicities of organophosphate, phthalimide, pyrethroid and carbamate insecticides by the Ames and lactam tests. *Mutagenesis* 13:157–166
81. Zahran MM, Abdel-Aziz KB, Abdel-Raof A, Nahas EM (2005) The effect of subacute doses of organophosphorus pesticide, Nuvacron, on the biochemical and cytogenetic parameters of mice and their embryos. *Res J Agric Biochem Sci* 1:277–283